



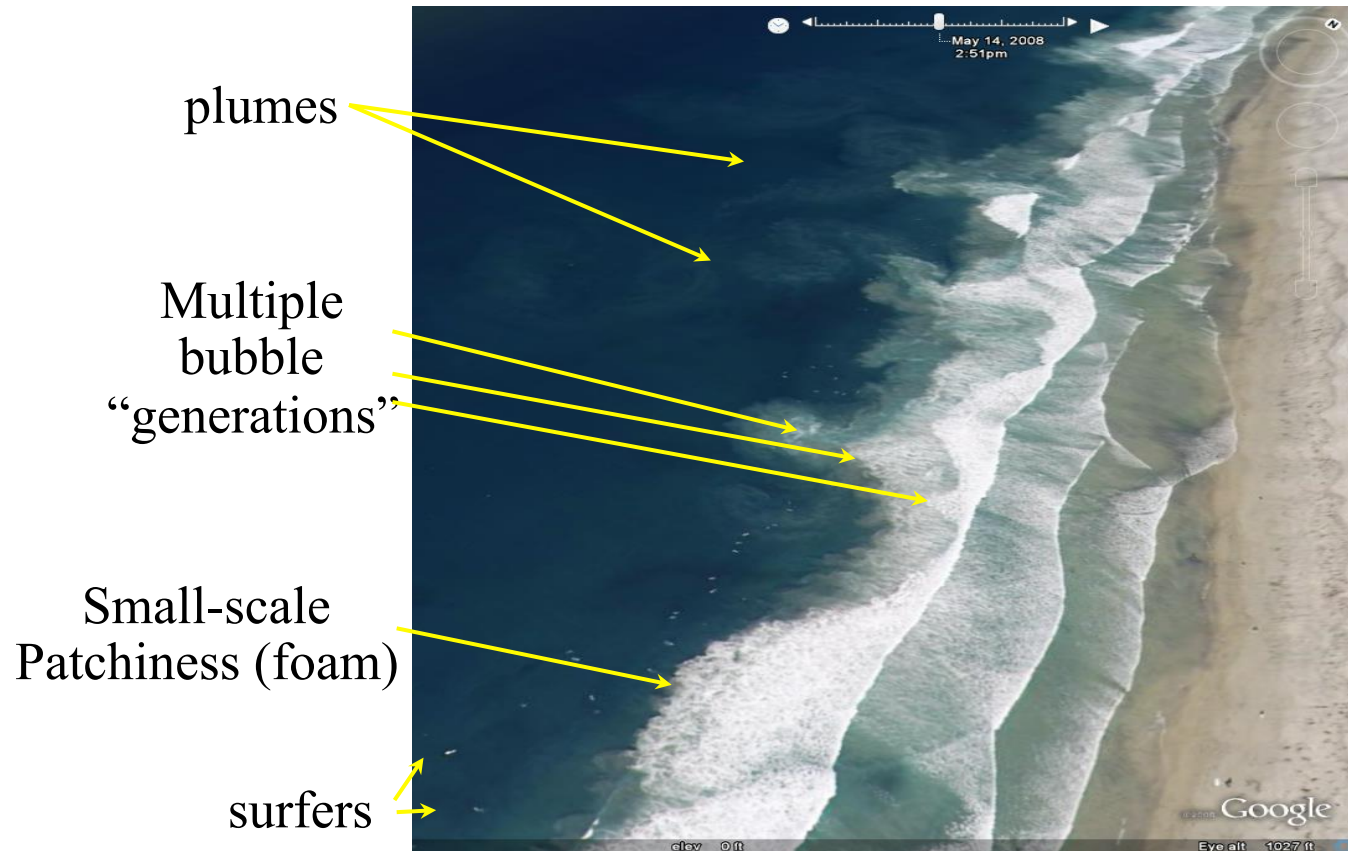
*Turbulent coherent structures, mixing and
bubble entrainment under surf zone
breaking waves*

**James T. Kirby, Gangfeng Ma,
Morteza Derakhti and Fengyan Shi**

**Center for Applied Coastal Research
University of Delaware**

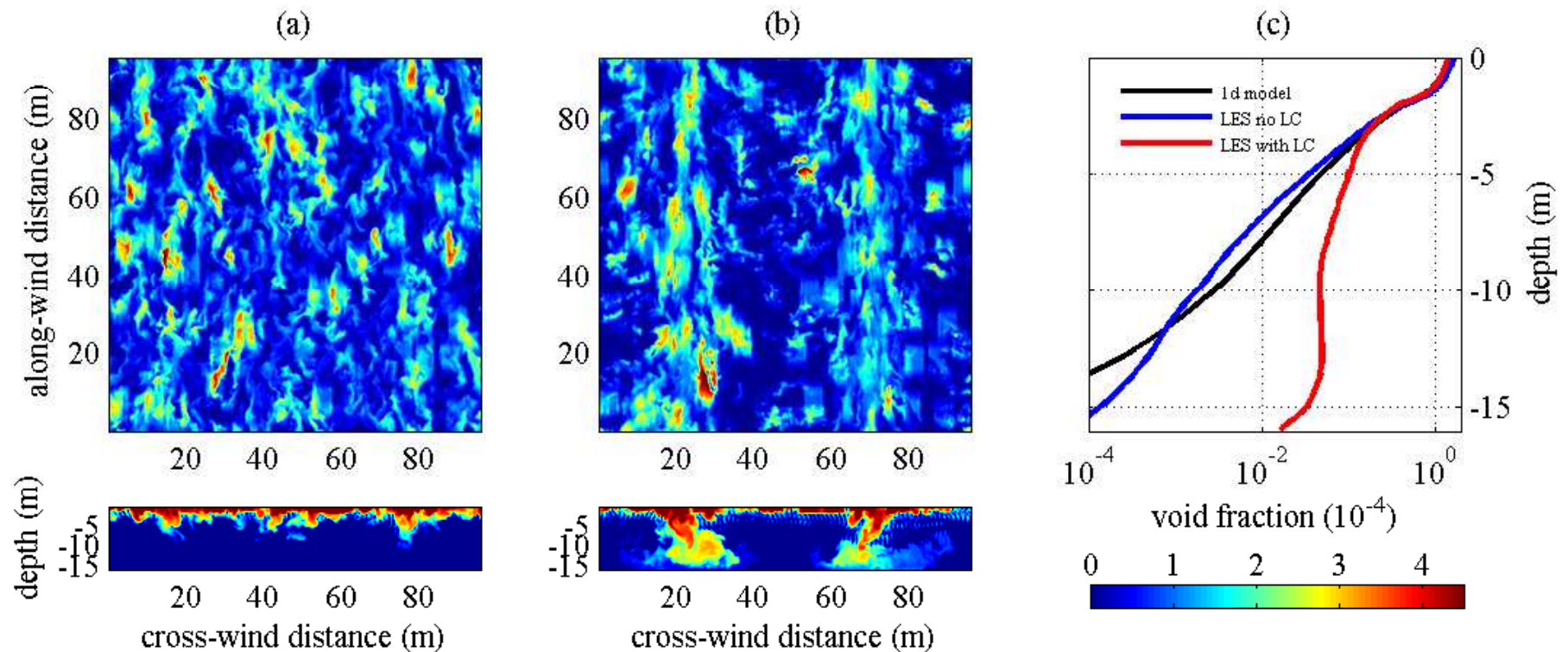
Motivation

Optical and acoustic properties of surf zone (both wave-averaged and inter-wave)



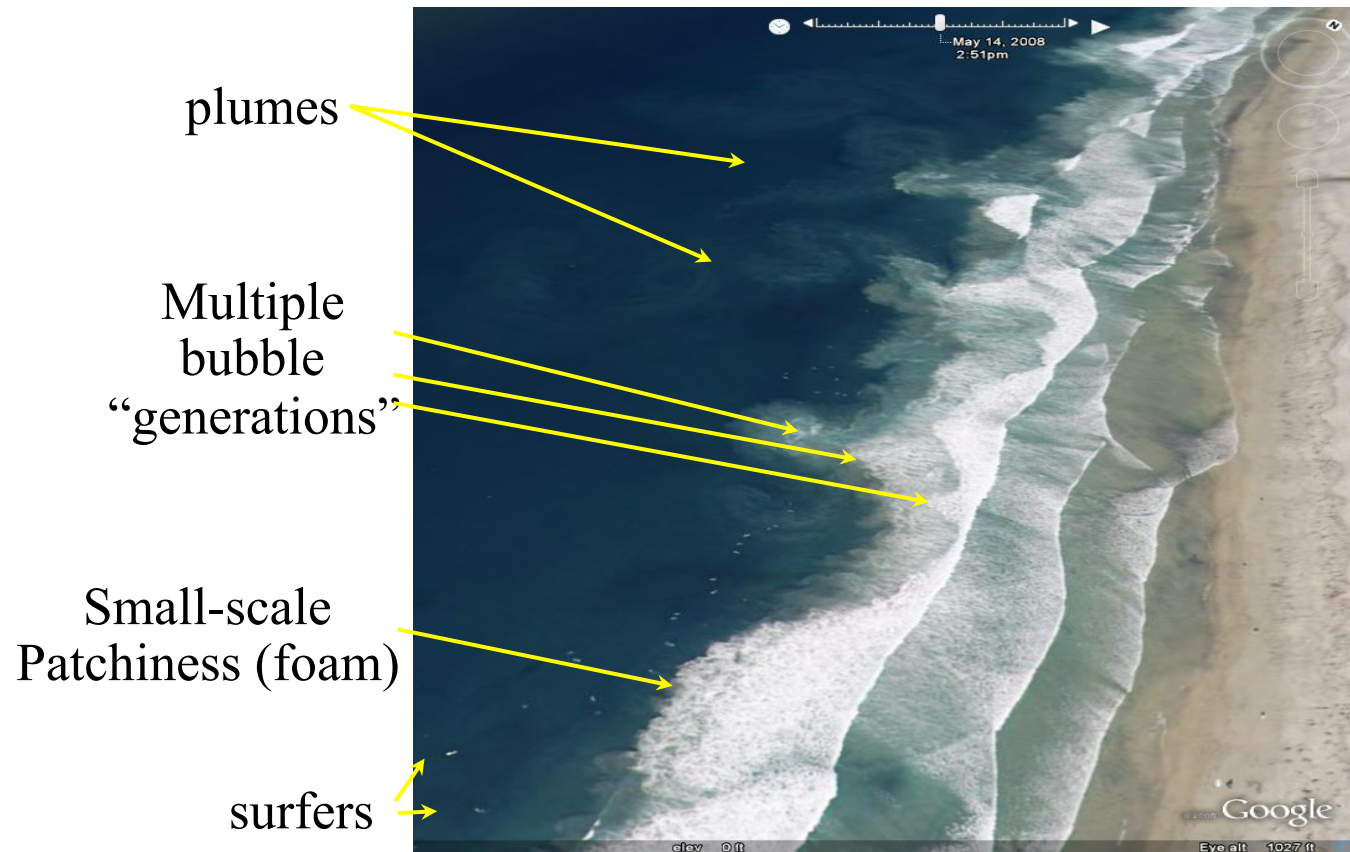
- Gas exchange problem at air-sea interface





Instantaneous three dimensional void fraction distribution determined from an LES without (a) and with (b) LC effects, horizontal plane at $z = -1.5$ m (top) and a crosswind-depth section at arbitrary along-wind location (bottom, in log scale for visual enhancement). (Kukulka and Kirby, 2012)

Surf Zone Optical Constituent Dynamics : Wave-Induced Bubbles & Foam



Can bubble generation and transport be modeled as a function of wave energy input and bathymetry?

How are bubbles entrained into the water column?

Goals:

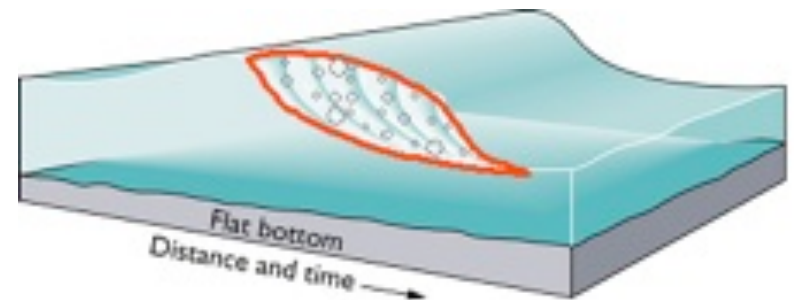
- Develop a model for instantaneous bubble distribution under surf zone breaking waves;
- Investigate interaction between void fraction and turbulence properties;
- Formulate a model for wave-driven circulation (longshore and rip currents, large-scale vortices), resulting bubble distribution and transport, and generation and transport of foam on the water surface.

What are the dominant mechanisms for bubbly flow?

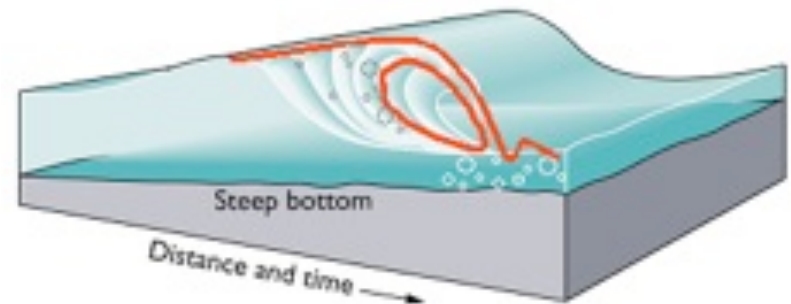
- Turbulence generation and bubble entrainment at the free surface;
- Bubbles with different sizes, Stokes number $St \sim O(1)$;
- Void fraction up to 20~30%;
- Intense interactions among bubbles, mean flow and turbulence;
- Bubble breakup and coalescence

Methodology:

- Polydisperse Eulerian-Eulerian two-fluid approach;
- Volume-of-Fluid (VOF) approach to capture complex free surface during wave breaking



(a) SPILLING BREAKER



(b) PLUNGING BREAKER

Polydisperse Two-fluid Model for Bubbly Flows (Carrica et al., 1999; Ma et al., 2011)

$$\frac{\partial(\alpha_l \rho_l)}{\partial t} + \nabla \cdot (\alpha_l \rho_l \mathbf{u}_l^V) = 0$$

$$\frac{\partial(\alpha_l \rho_l \mathbf{u}_l^V)}{\partial t} + \nabla \cdot (\alpha_l \rho_l \mathbf{u}_l^V \mathbf{u}_l^V) = -\nabla p + \left(\alpha_l \rho_l + \sum_{i=1}^{NG} \alpha_{g,i} \rho_g \right) \mathbf{g} + \nabla \cdot \left[\alpha_l \boldsymbol{\mu}_{eff,l} (\nabla \mathbf{u}_l^V + \nabla^T \mathbf{u}_l^V) \right]$$

$$\frac{\partial N_{g,i}}{\partial t} + \nabla \cdot (\mathbf{u}_{g,i}^V N_{g,i}) = S_{N_{g,i}}$$

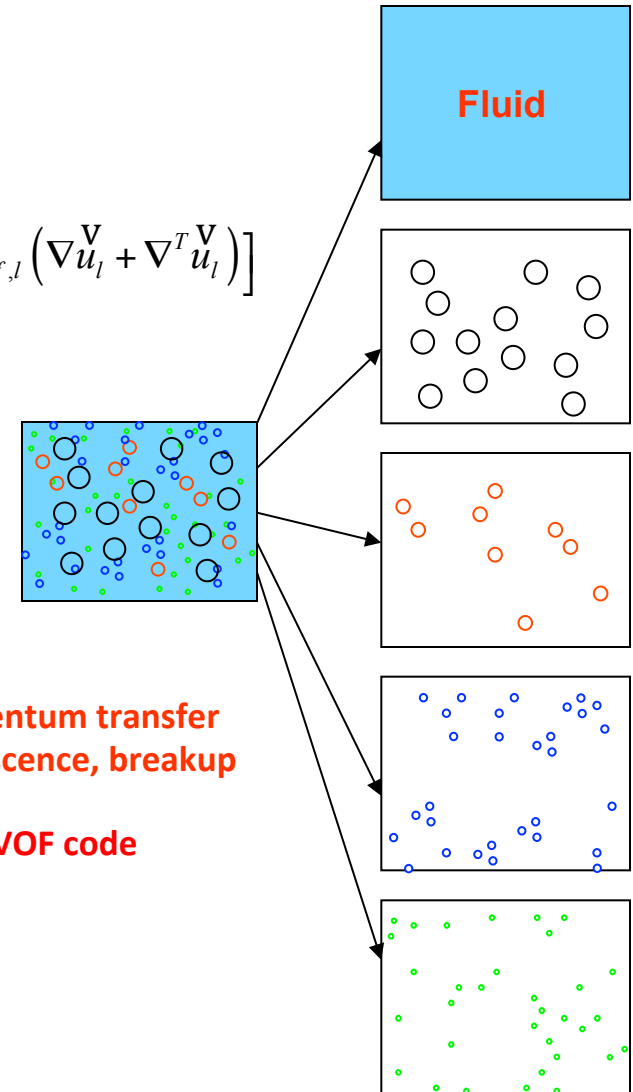
$$-\alpha_{g,i} \nabla p + \alpha_{g,i} \rho_g \mathbf{g} + M_{lg,i} = 0$$

$$\alpha_{g,i} = \frac{m_{g,i} N_{g,i}}{\rho_{g,i}}$$

$$\alpha_l + \sum_{i=1}^{NG} \alpha_{g,i} = 1$$

$$M_{gl} = -\sum_{i=1}^{NG} M_{lg,i}$$

Forces on bubble phase include lift force, drag force and added mass force



Turbulence Models

- **2-D: Two phase k - ϵ for bubbly flow (Troshko & Hassan, 2001)**
- Source term in TKE equation includes drag force effects
- Bubble effects on turbulent dissipation rate

$$\frac{\partial(\alpha_l \rho_l k)}{\partial t} + \nabla \cdot (\alpha_l \rho_l \mathbf{u}_l k) = \nabla \cdot \left(\alpha_l \frac{\mu_{T,l}}{\sigma_k} \nabla k \right) + \alpha_l (P - \rho_l \epsilon) + S_{bk}$$

$$\frac{\partial(\alpha_l \rho_l \epsilon)}{\partial t} + \nabla \cdot (\alpha_l \rho_l \mathbf{u}_l \epsilon) = \nabla \cdot \left(\alpha_l \frac{\mu_{T,l}}{\sigma_\epsilon} \nabla \epsilon \right) + \alpha_l \left(C_{\epsilon 1} \frac{\epsilon}{k} P - C_{\epsilon 2} \rho_l \frac{\epsilon^2}{k} \right) + S_{b\epsilon}$$

- **3-D: Two phase LES**
- Bubble-induced viscosity (Sato & Sekoguchi, 1975)
- Smagorinsky sub-grid model for turbulent eddy viscosity

$$\mu_{eff,l} = \mu_{L,l} + \mu_{T,l} + \mu_{BIT,l} \quad \mu_{T,l} = \rho_l (C_s \Delta)^2 |\mathbf{S}|$$

$$\mu_{BIT,l} = \rho_l C_{\mu,BIT} \sum_{i=1}^{NG} \alpha_{g,i} d_{bi} |\mathbf{u}_r|$$

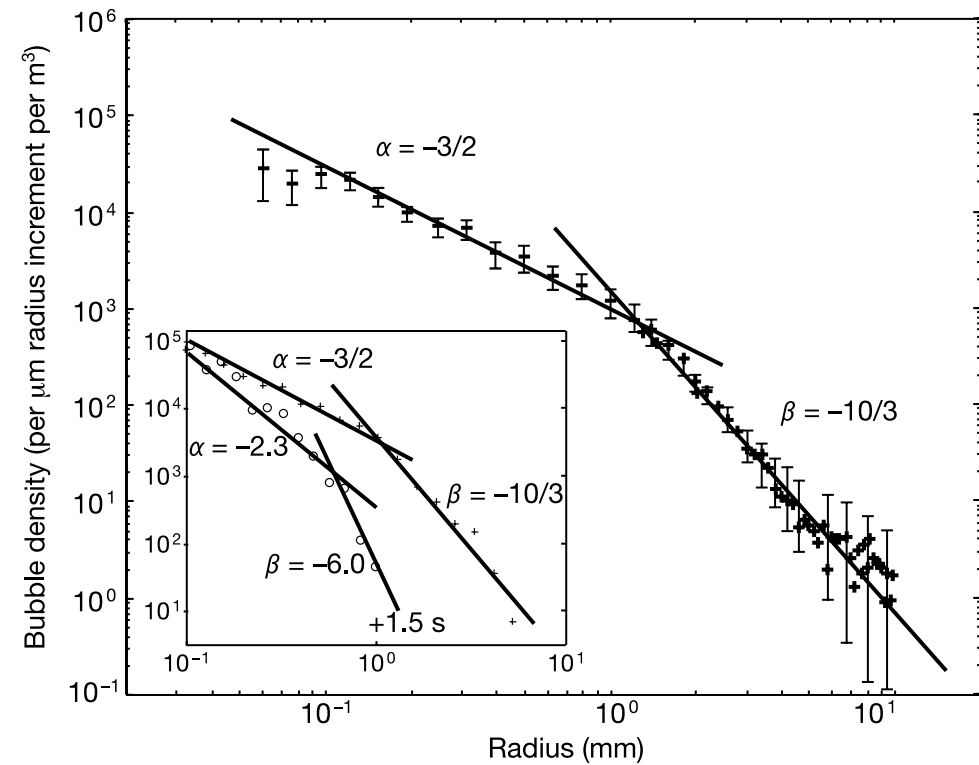
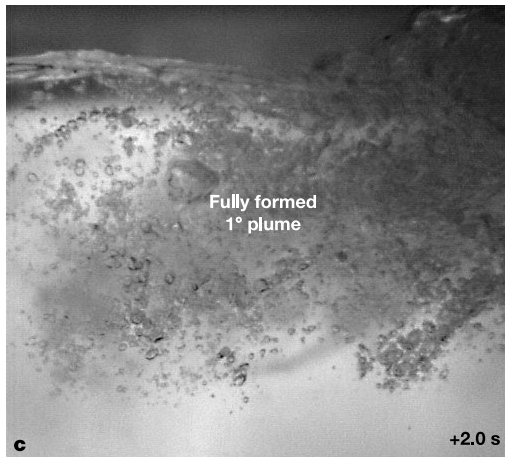
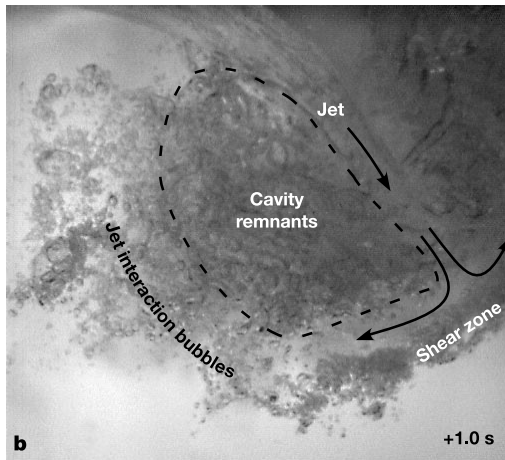
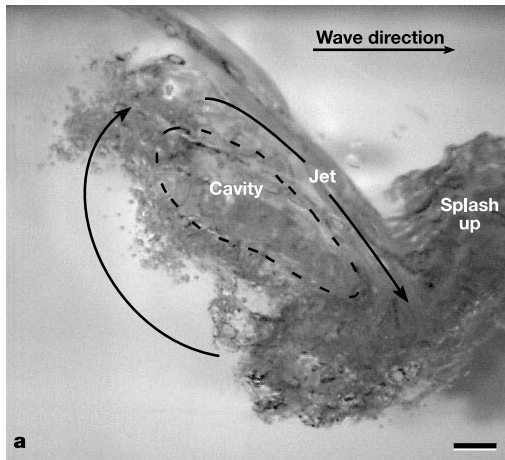
Bubble generation mechanisms:

- Cavity capture and collapse
- Continuous bubble entrainment through turbulent surface folding processes

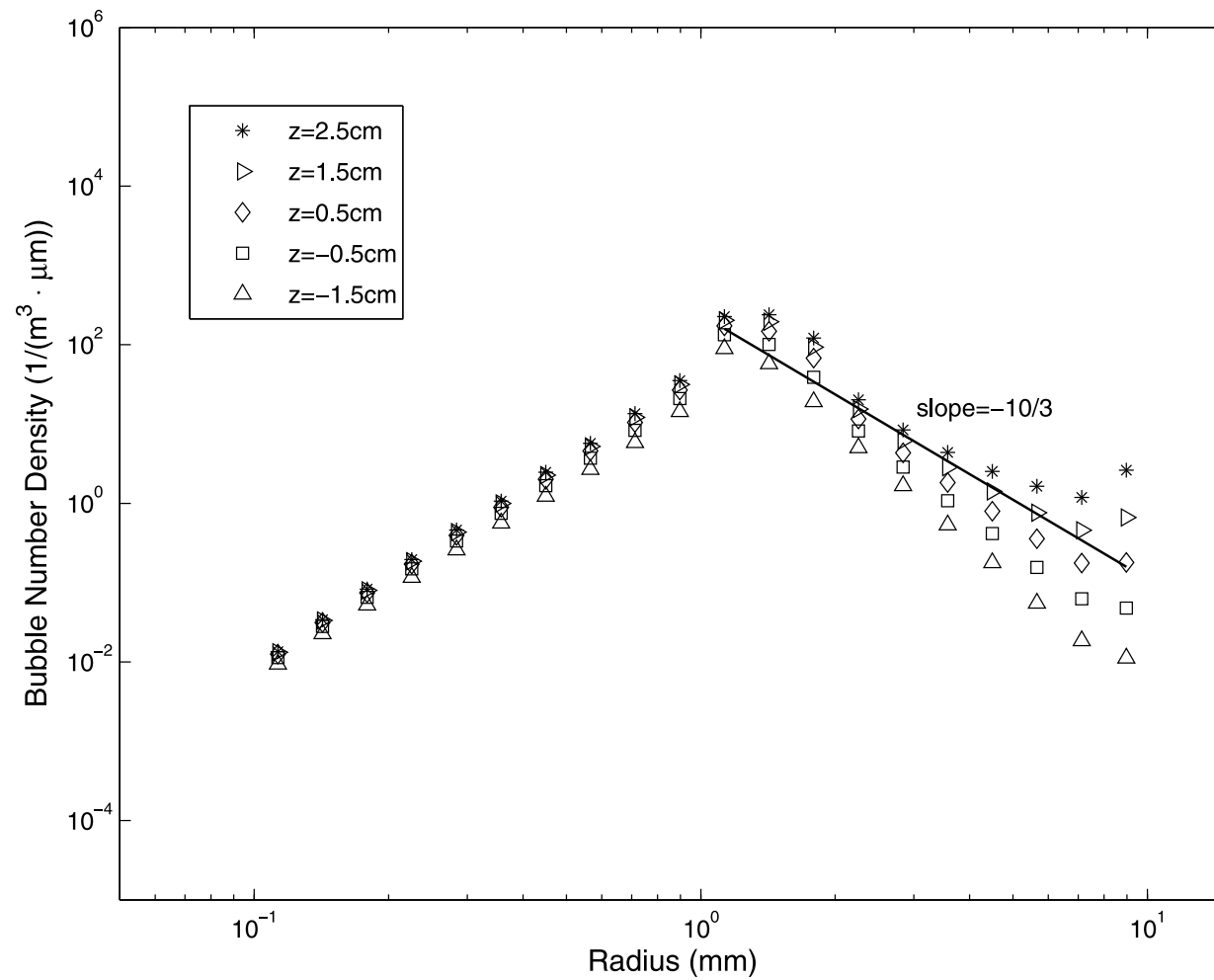
Source terms in bubble number density equation:

- Bubble breakup: Model of Martinez-Bazán et al (1999a,b, 2010)
- Bubble coalescence: ignored
- Bubble dissolution: ignored

Deane and Stokes (2002): Breakup of trapped cavity and resulting size distribution of bubbles



Model prediction of bubble size distribution based only on breakup mechanism. All bubbles initially have $D=9\text{mm}$



Bubble Entrainment Model

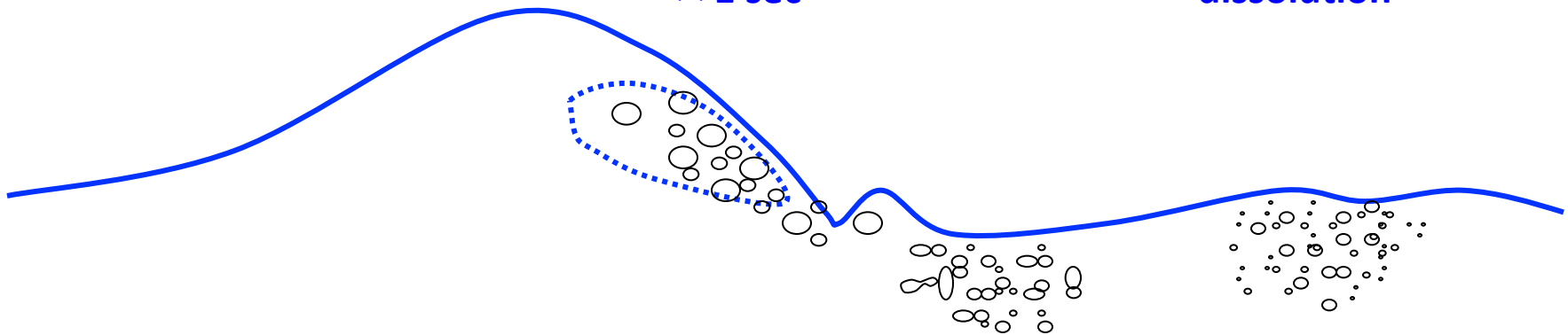
Deane and Stokes,
Nature, 2002

Acoustically active phase

- Jet/wave-face interaction
- Cavity collapse
- Primary plume formation
- $\ll 1$ sec

Quiescent phase

- Advection
- Turbulent diffusion
- buoyant degassing
- dissolution



Bubble entrainment rate is linearly
proportional to turbulent dissipation
rate (Ma et al., 2011)

$$B_{g,i} = \frac{c_b}{4\pi} \left(\frac{\sigma}{\rho_l}\right)^{-1} \alpha_l \frac{f(a_i) \Delta a_i}{\sum_{i=1} a_i^2 f(a_i) \Delta a_i} \epsilon$$

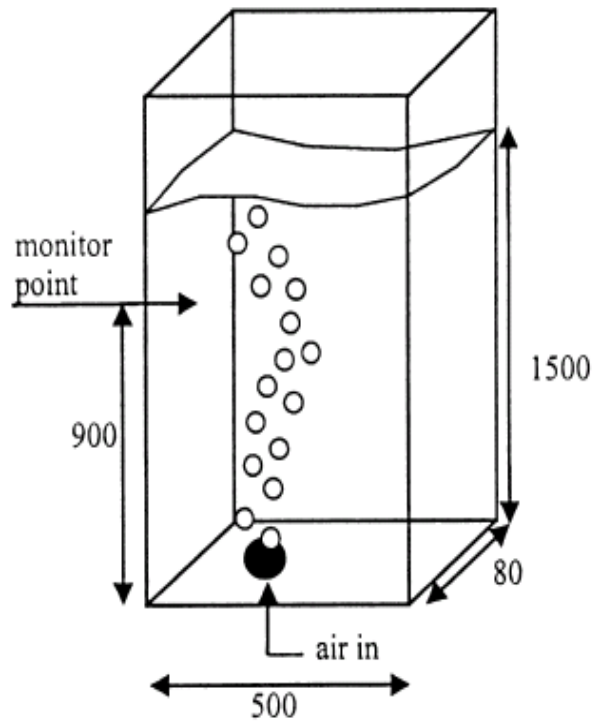
Bubble size spectrum by Deane
and Stokes (2002)

$$f(a) \propto a^{-10/3} \quad \text{if } a \geq 1.0 \text{ mm}$$

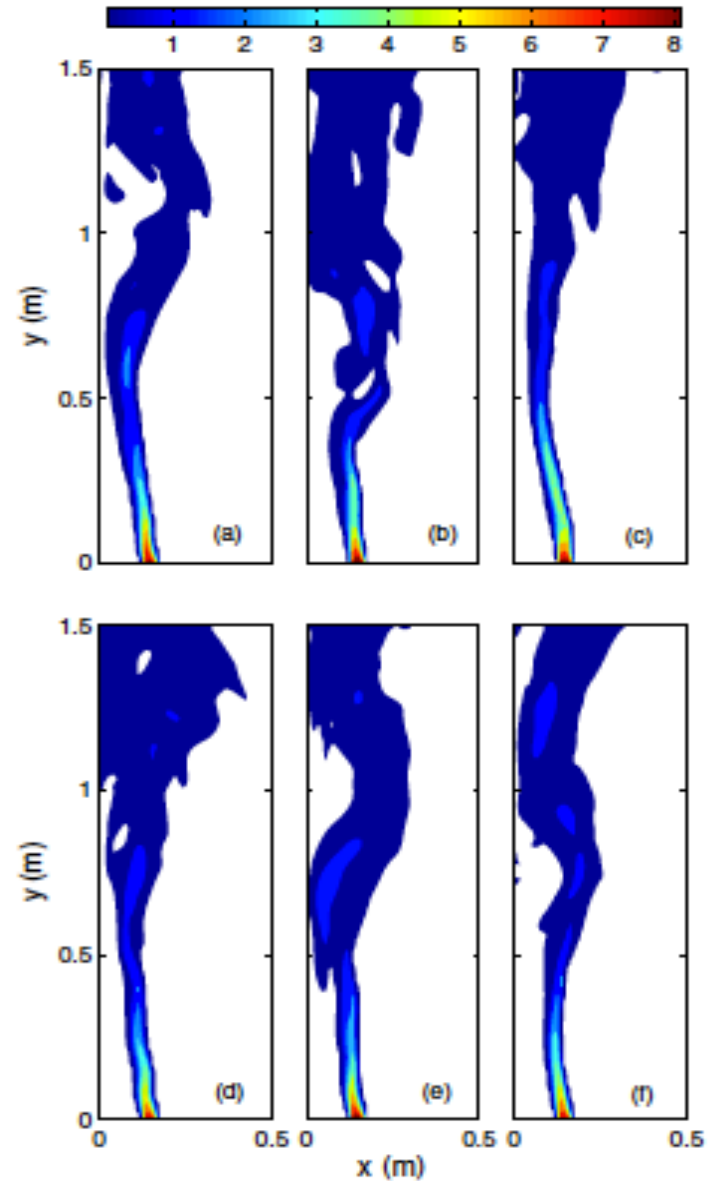
$$f(a) \propto a^{-3/2} \quad \text{if } a \leq 1.0 \text{ mm}$$

Hinze scale = 1.0 mm

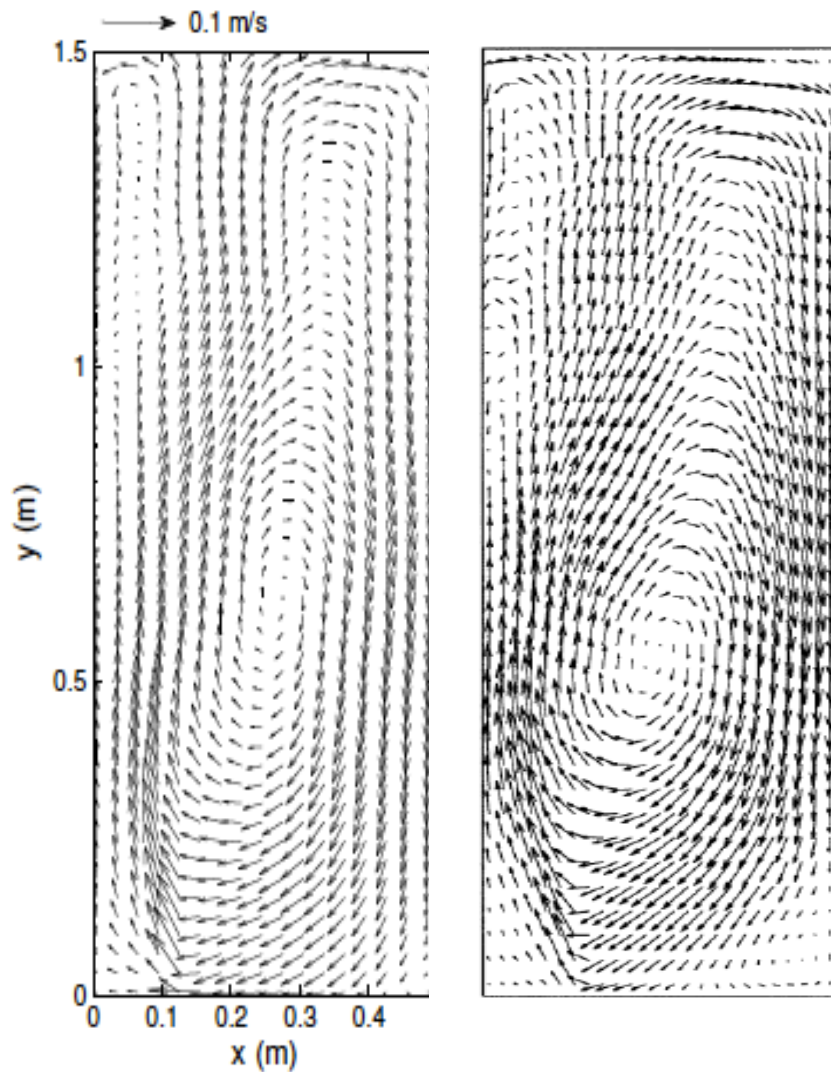
Oscillatory Bubble Plume



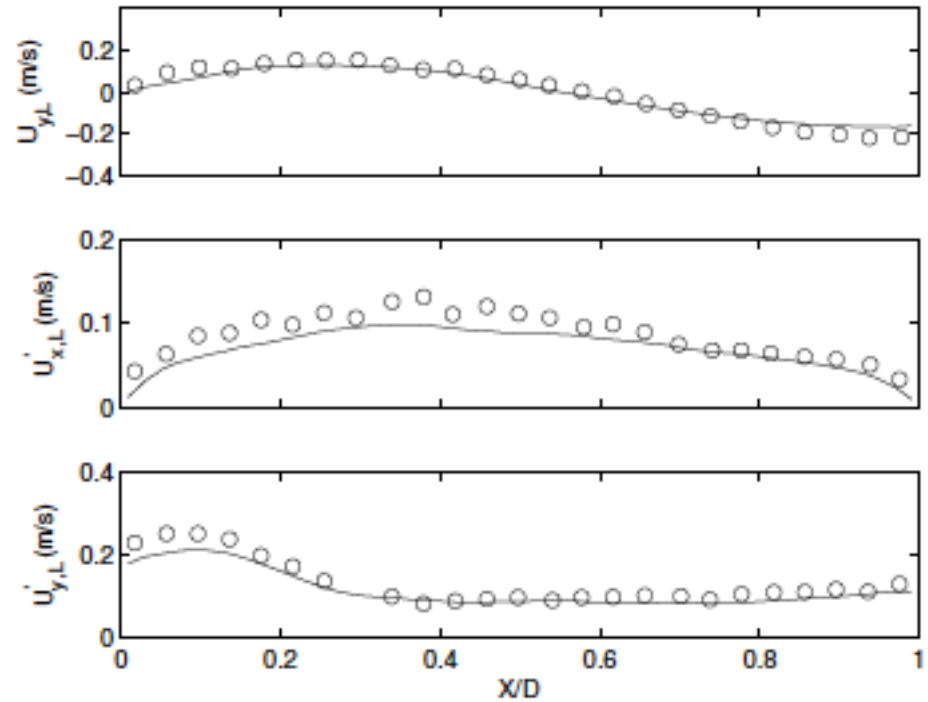
Laboratory experiment by
Becker et al., 1994



Simulated oscillatory bubble plume.
Time interval between snapshots is 10 sec.



Model-data comparison of time averaged liquid phase velocity (left: simulation; right: measurement)



Model-data comparisons of time averaged liquid phase velocity and velocity fluctuations at $y = 1050$ cm (lines: simulation; circles: measurement)

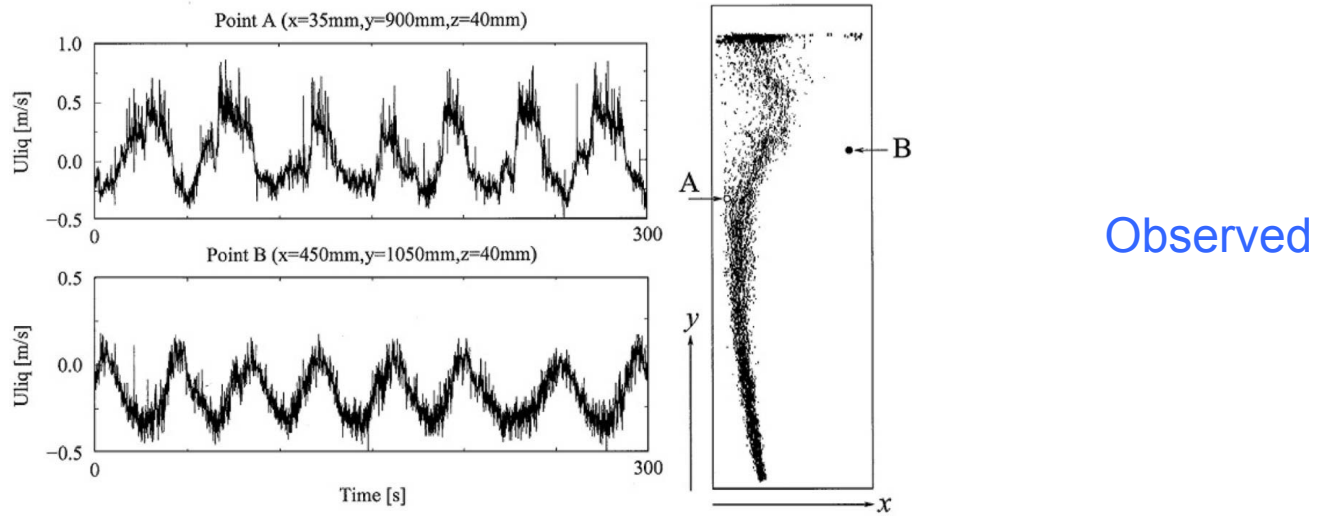


Figure 1. Local transient measurements of the vertical liquid velocity at positions A (bubbly flow) and B (bubble free zone) (reprinted from *Sokolichin and Eigenberger [1999]* with permission from Elsevier).

Oscillation in bubble plume:
 Simulated

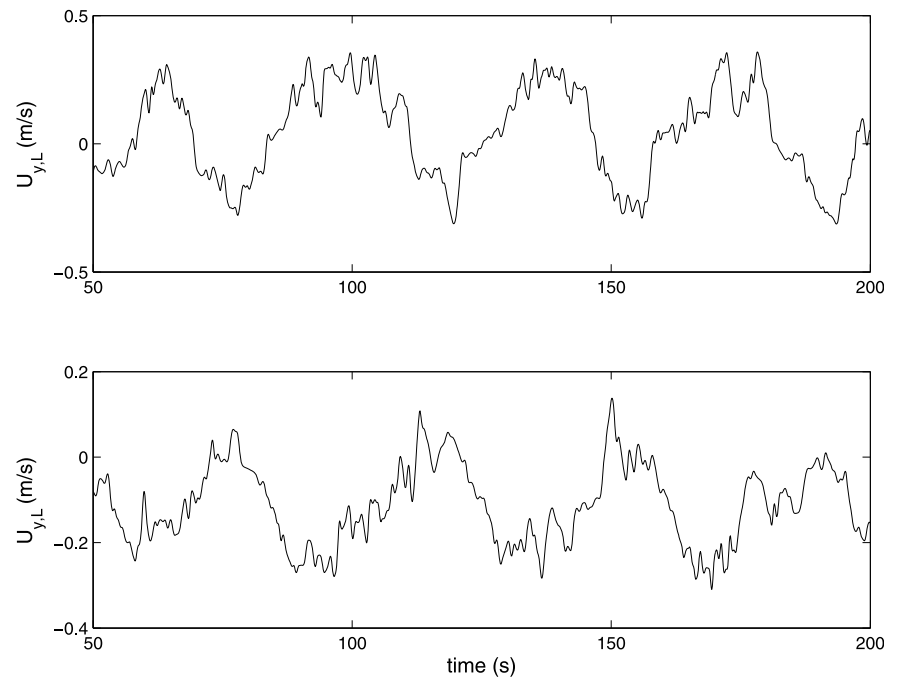
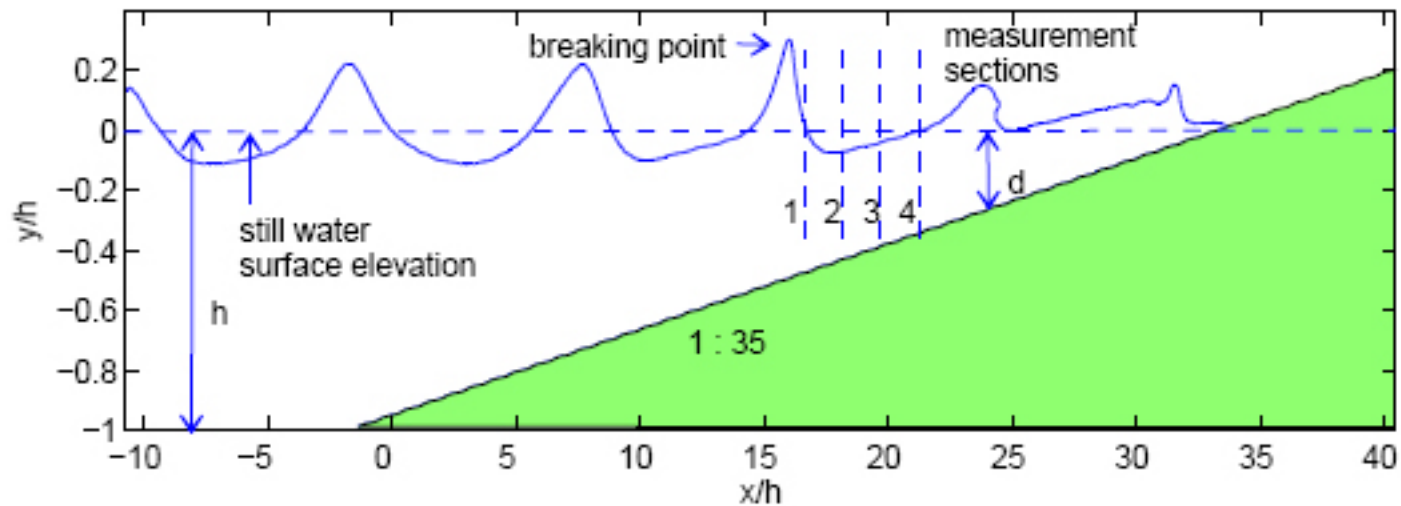
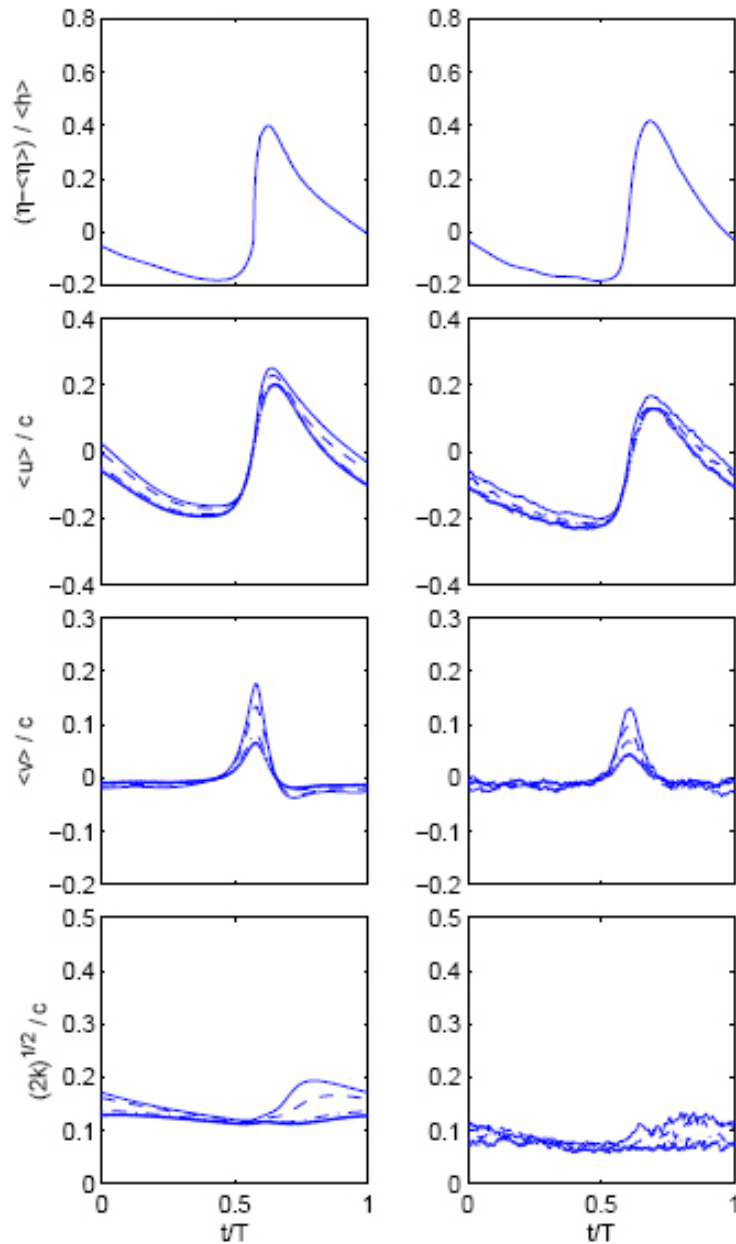


Figure 4. Simulated time series of vertical liquid velocity at monitor point (top) A and (bottom) B.

Model Validation II: Turbulence under breaking waves

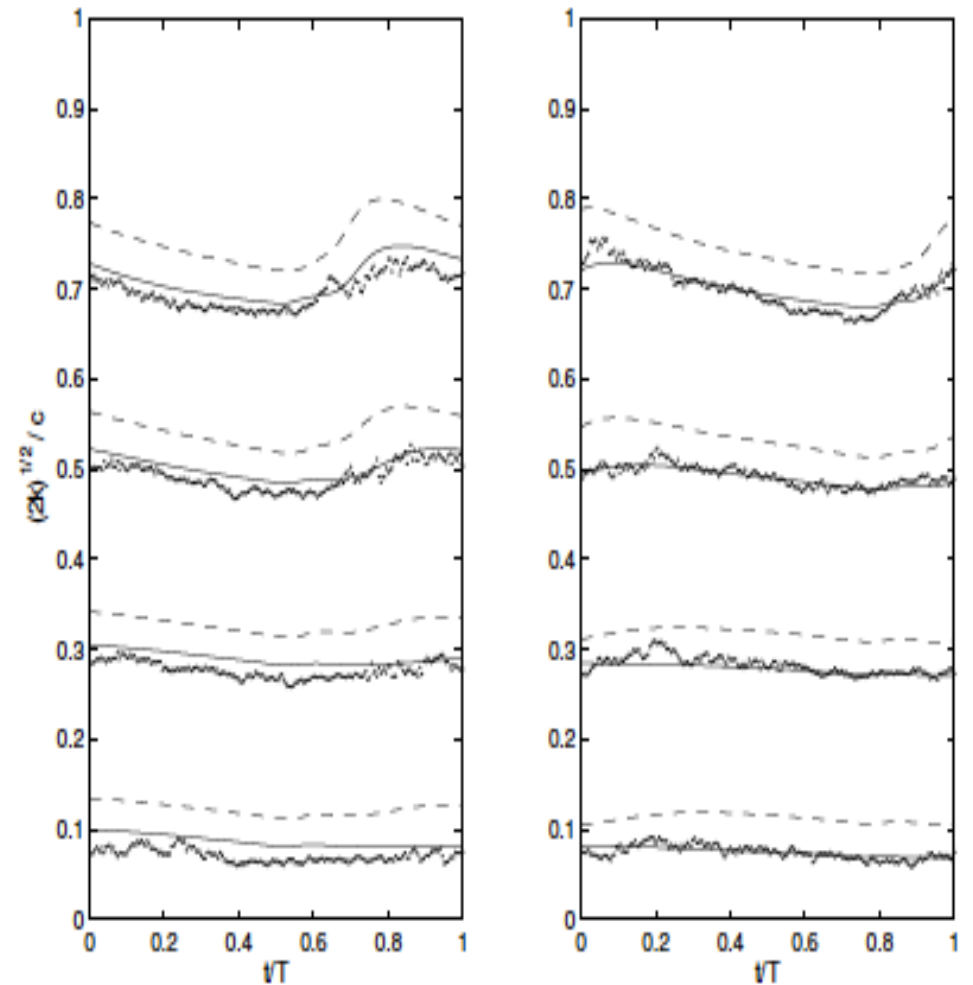


Laboratory experiment by Ting & Kirby (1994, 1996)
Spilling breaking wave
Simulations with and without bubbles



simulations

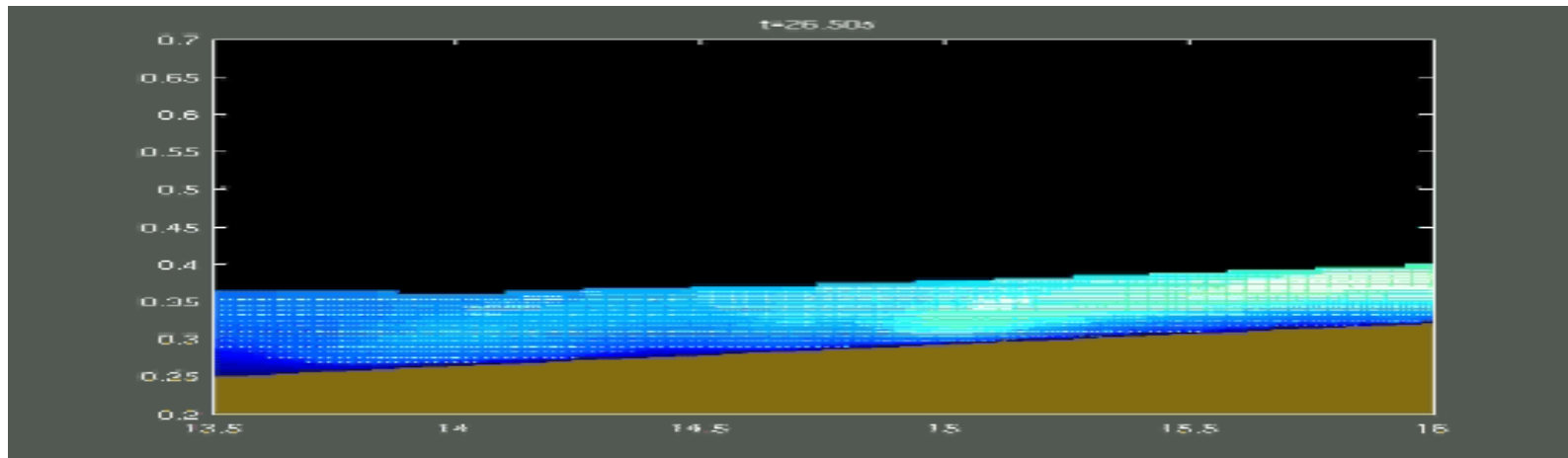
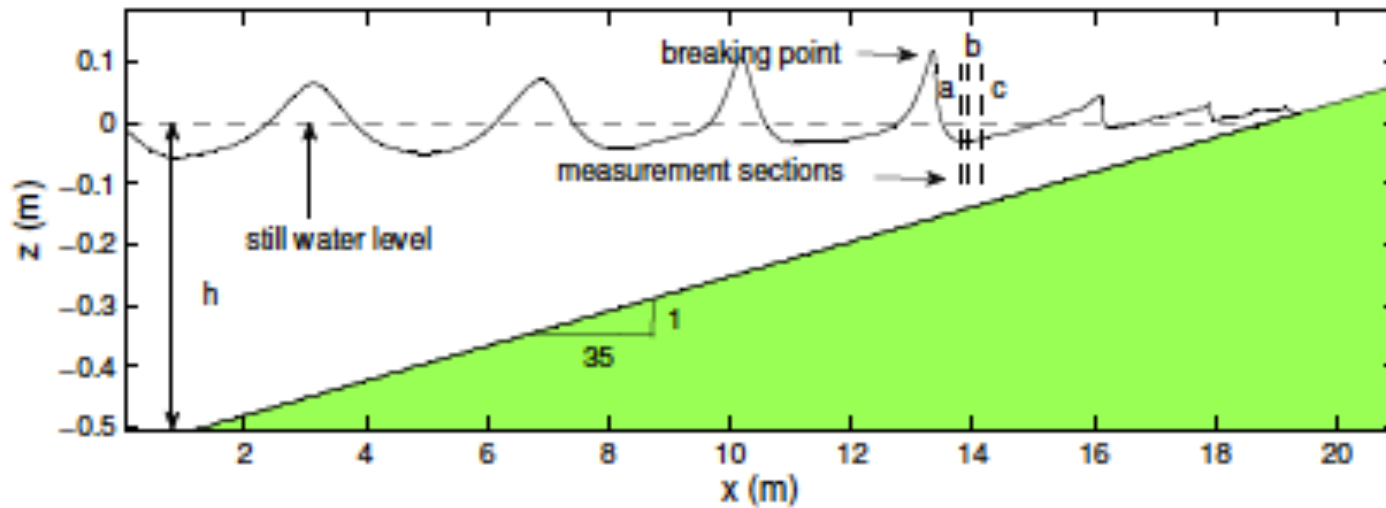
measurements



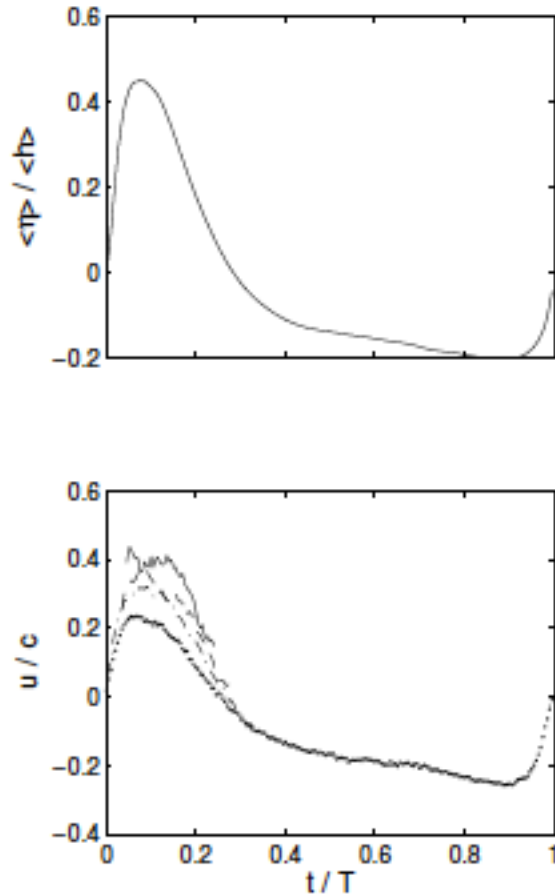
Model-data comparisons of TKE with (solid lines) and without (dashed lines) bubbles. Dotted-lines: measurements

Part I: Void Fraction Evolution and Distribution (Ma et al., JGR, 2011)

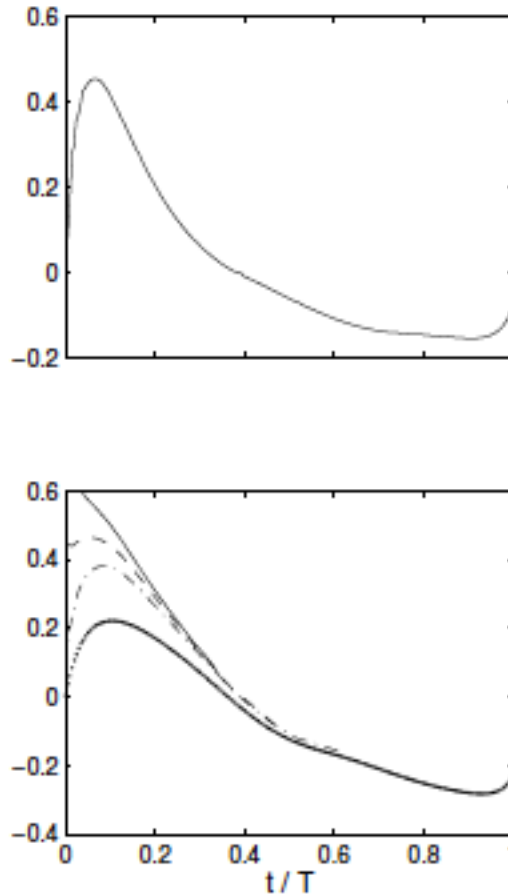
Laboratory experiment
by Cox & Shin (2003)



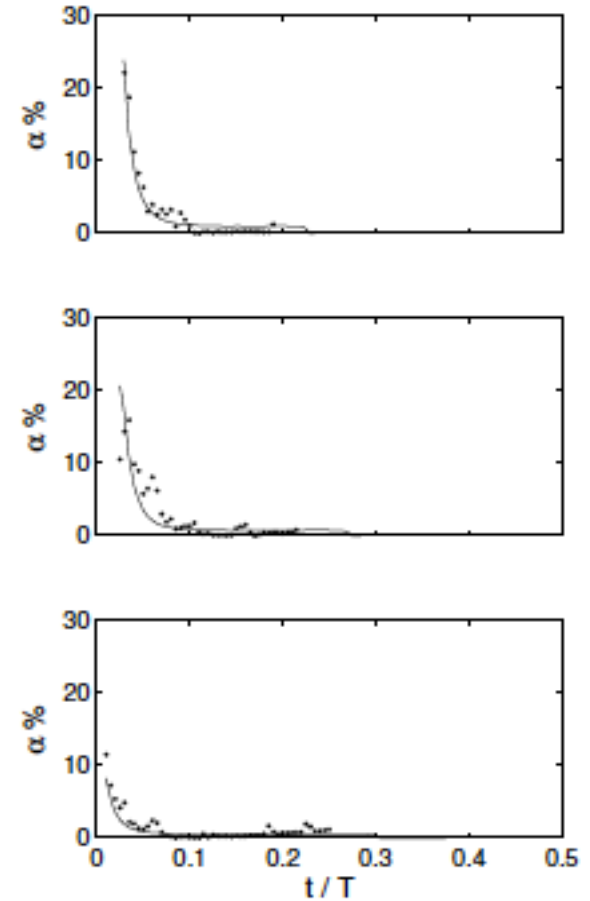
Model-data comparisons of free surface elevation, streamwise velocity and void fraction at section 1



measurements



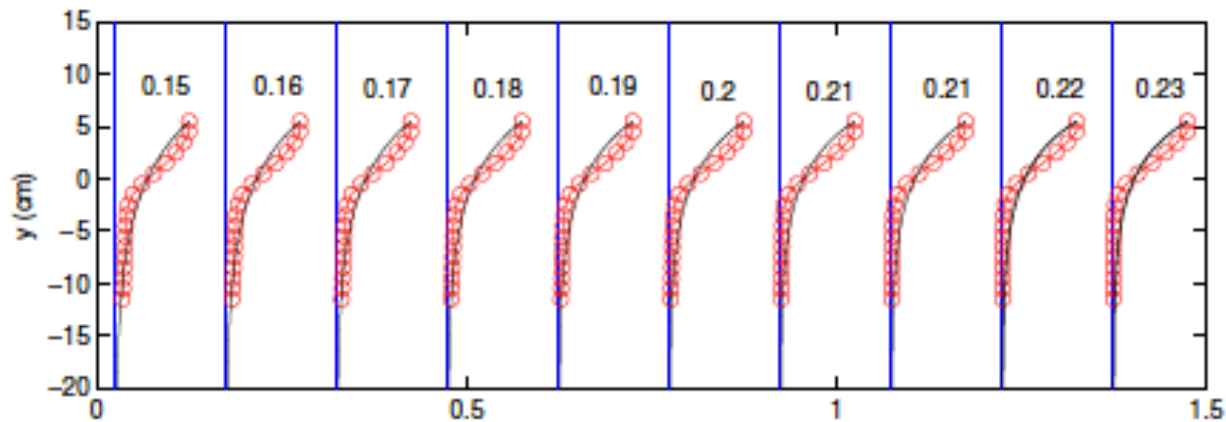
simulations



void fraction comparisons at three vertical locations

Vertical Distributions of Void Fraction

Smallest

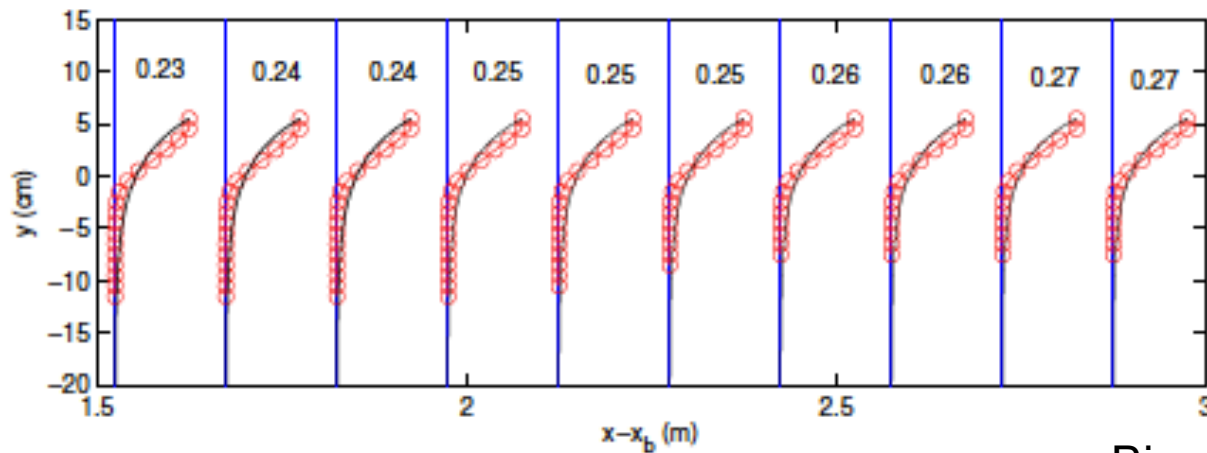


Exponential relationship:

$$C(z) = C_m \exp(k_z(z - z_m))$$

$$C(z) = C_m \quad z = z_m$$

$$C(z) \rightarrow 0 \quad z \rightarrow -\infty$$

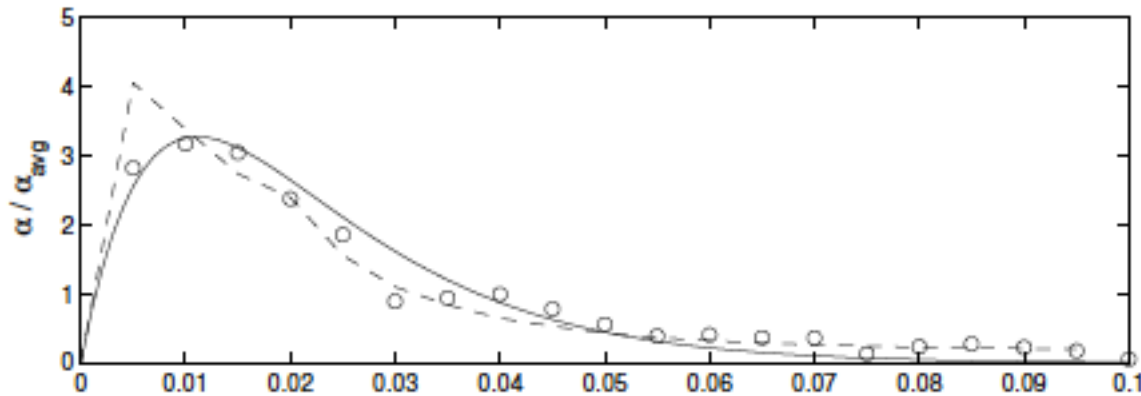


Circles:
simulations

Solid lines:
exponential fitting

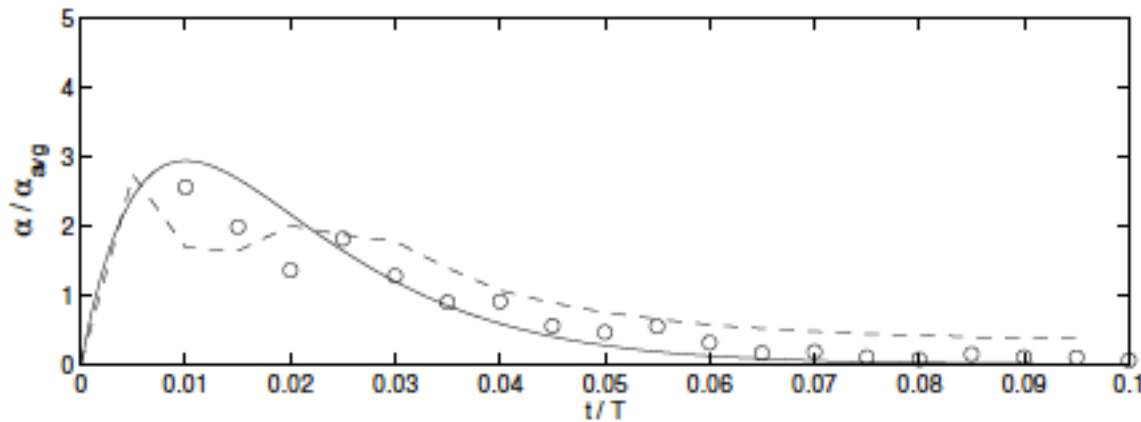
Biggest

Temporal Variations of Void Fraction



$$\frac{\alpha}{\alpha_{ave}} = a\left(\frac{t'}{T}\right)\exp\left[-b\left(\frac{t'}{T}\right)\right]$$

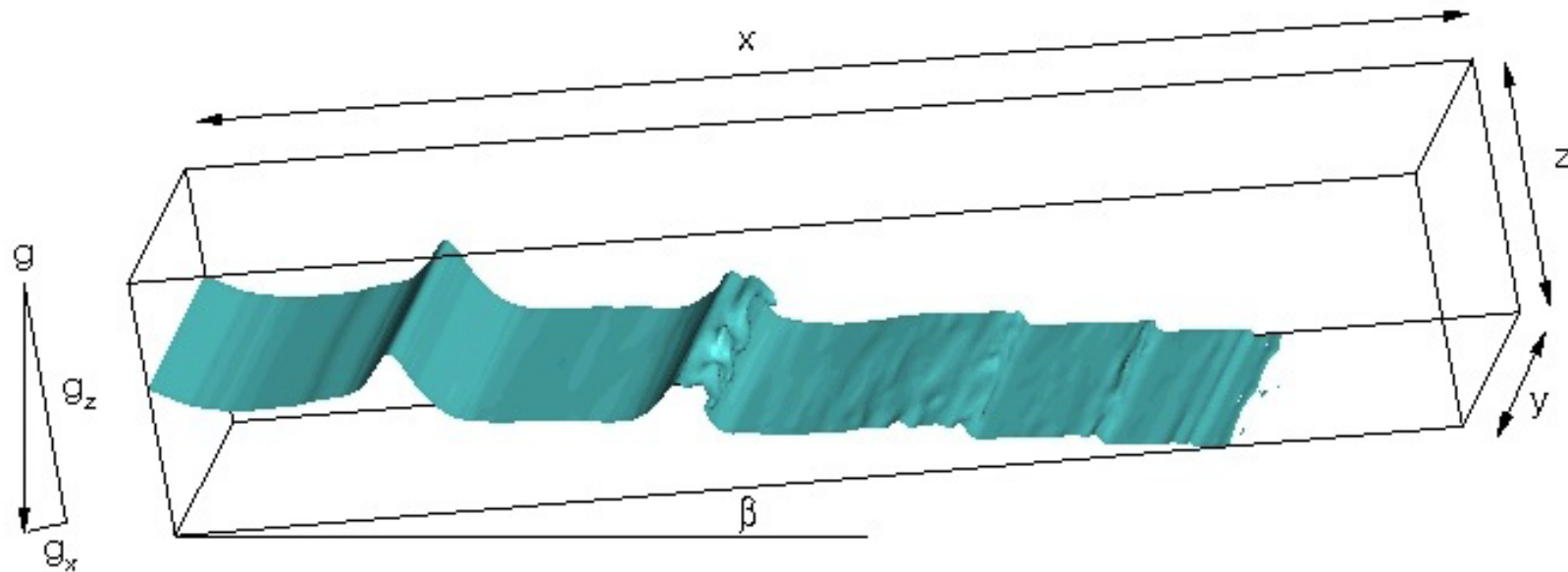
$$a = 800, b = 90$$



upper panel: above SWL
Lower panel: below SWL

Circles: measurements; dashed lines: simulations;
solid lines: emperical fitting

Turbulent Coherent Structures and their Interactions with Dispersed Bubbles



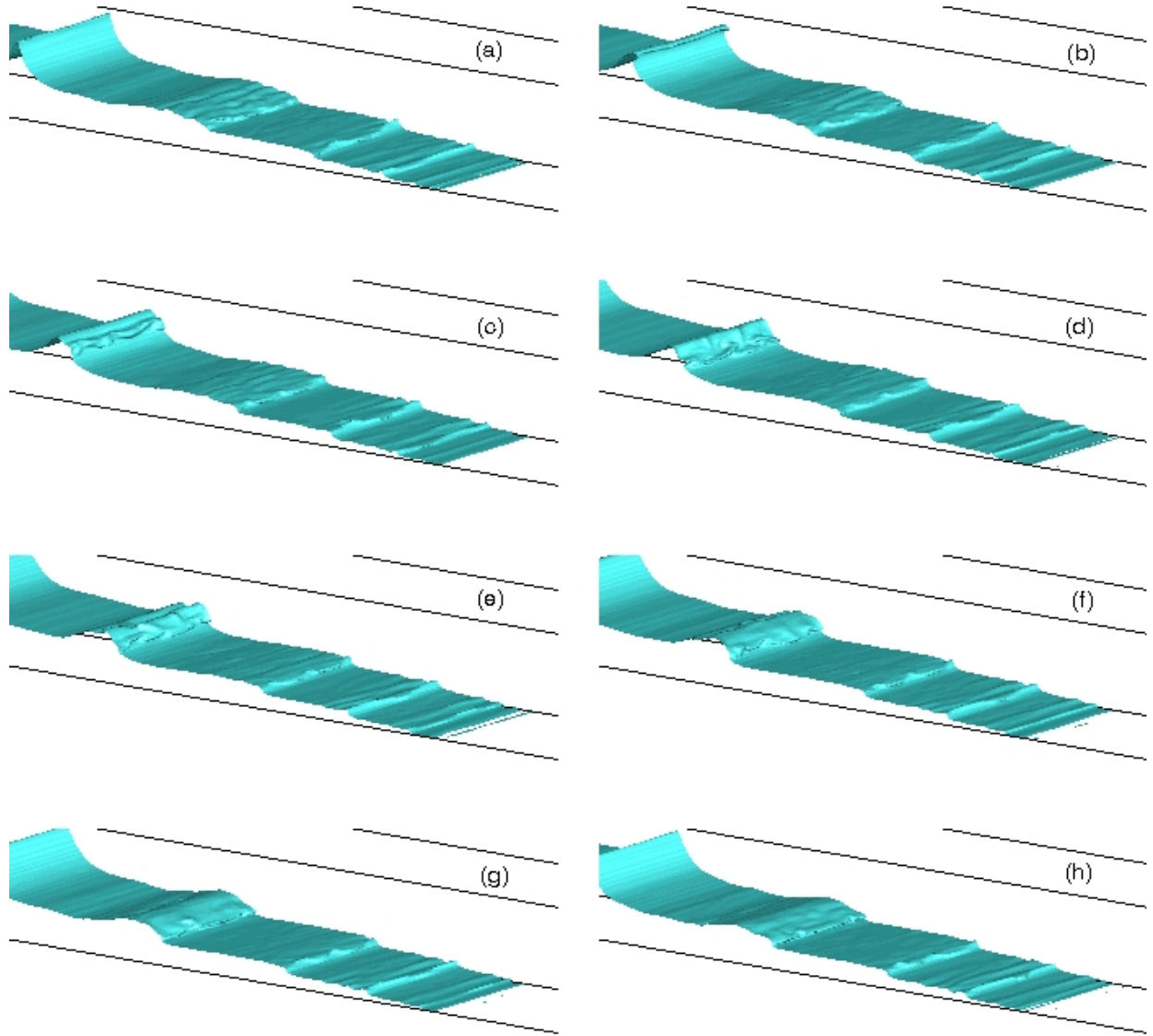
Spilling breaking wave (Ting and Nelson, 2011)

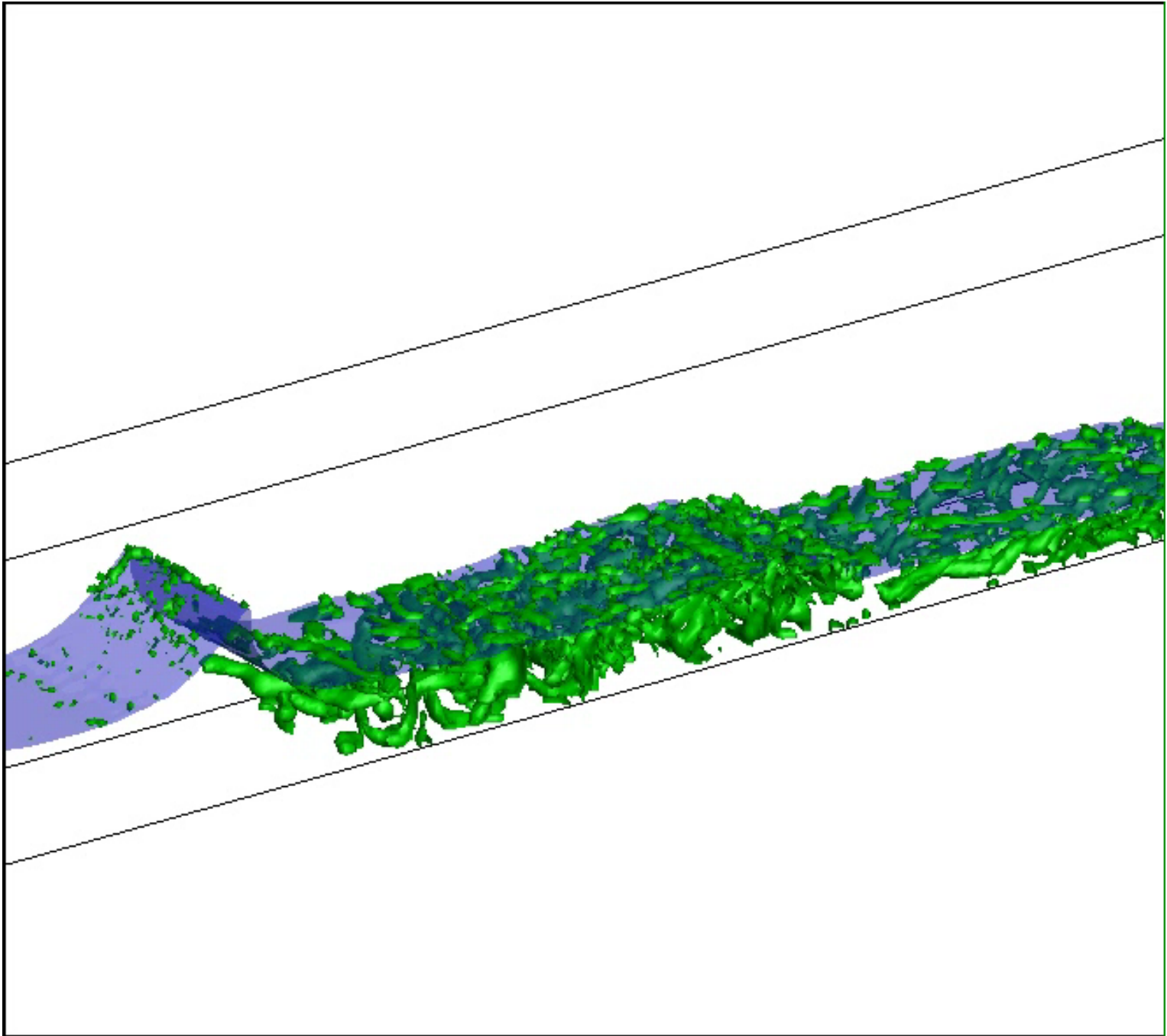
Domain size: 15m \times 0.3m \times 0.6m

Grid size: 0.04m \times 0.0075m \times 0.0075m

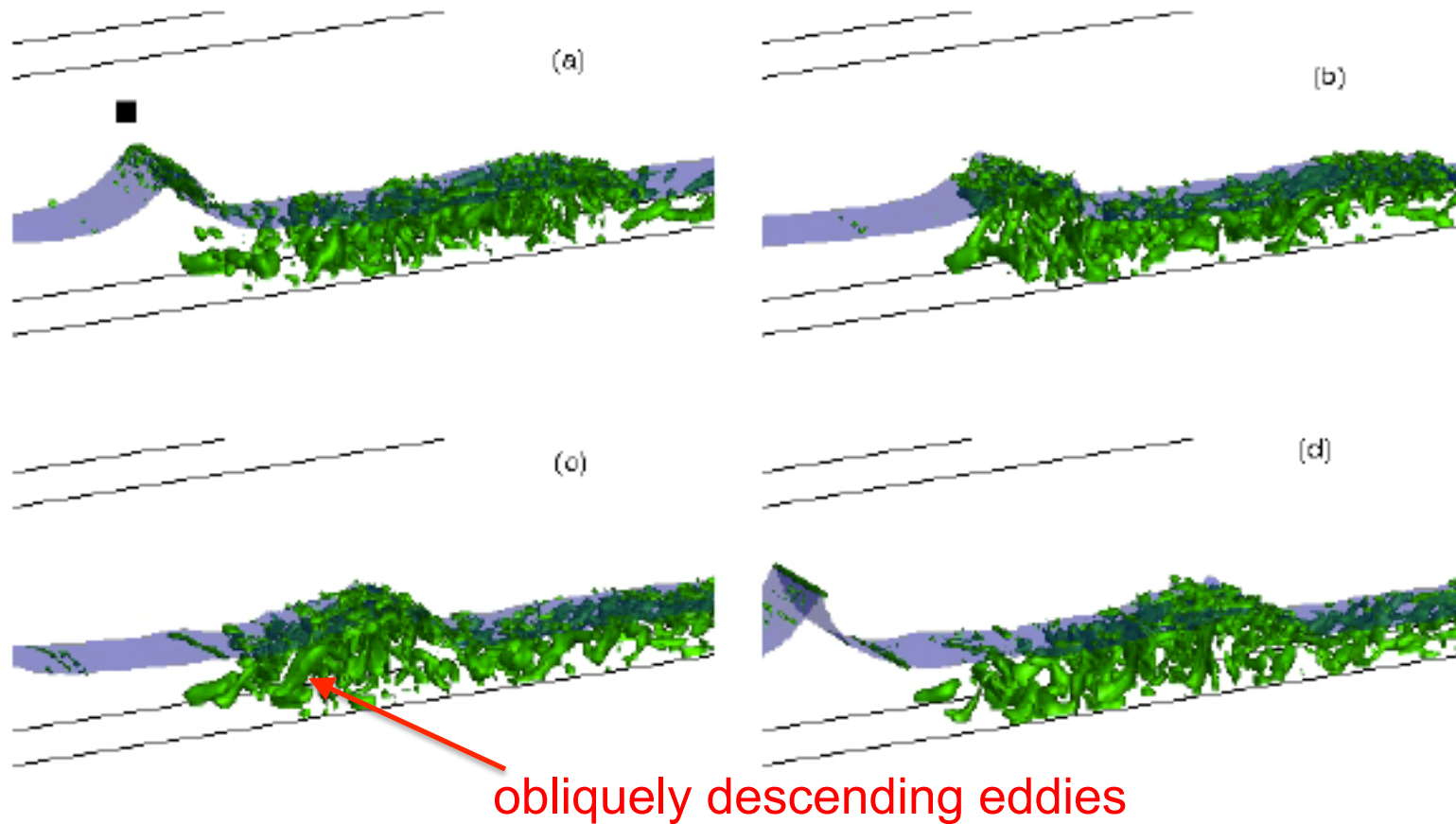
Bed slope: $\tan\beta = 0.03$

Evolution of Free Surface (Captured by VOF Approach)



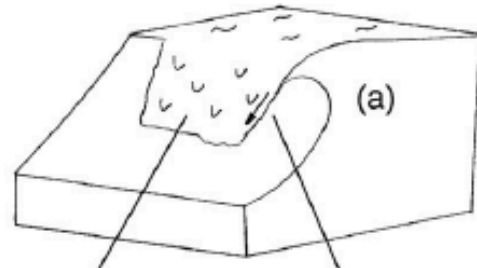


Turbulent Vortex Structures



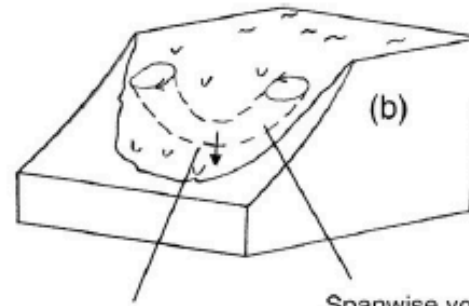
Evolution of vortex structures at (a) $t=t_b+1/8T$; (b) $t=t_b+3/8T$; (c) $t=t_b+5/8T$ and (d) $t=t_b+7/8T$. The vortex structures are recognized by the isosurfaces of $\lambda_2=-2.0$ (λ_2 is the second largest eigenvalue of the tensor $S^2+\Omega^2$).

Conceptual Model of obliquely descending eddies (Ting, 2008)



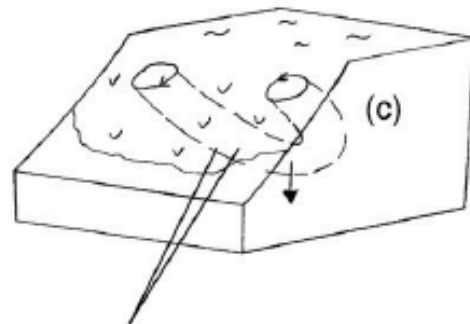
Falling water from non-uniform wave breaking

Air tube formed by plunging jet

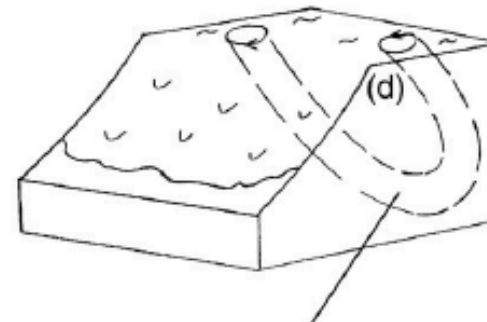


Non-uniform breaking causes part of vortex tube to descend faster than other

Spanwise vortex formed by plunging jet



As the lower part of vortex tube descends through the water column, higher translation velocity near the surface causes more stretching and bending



A vortex loop is left behind after the broken wave has passed

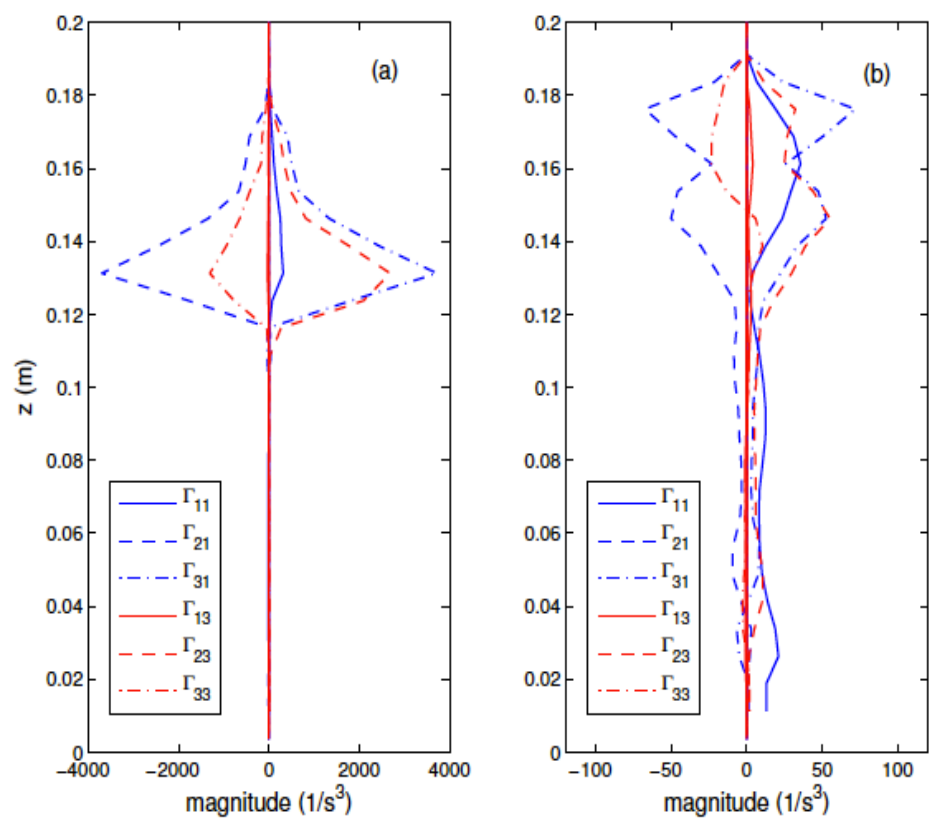
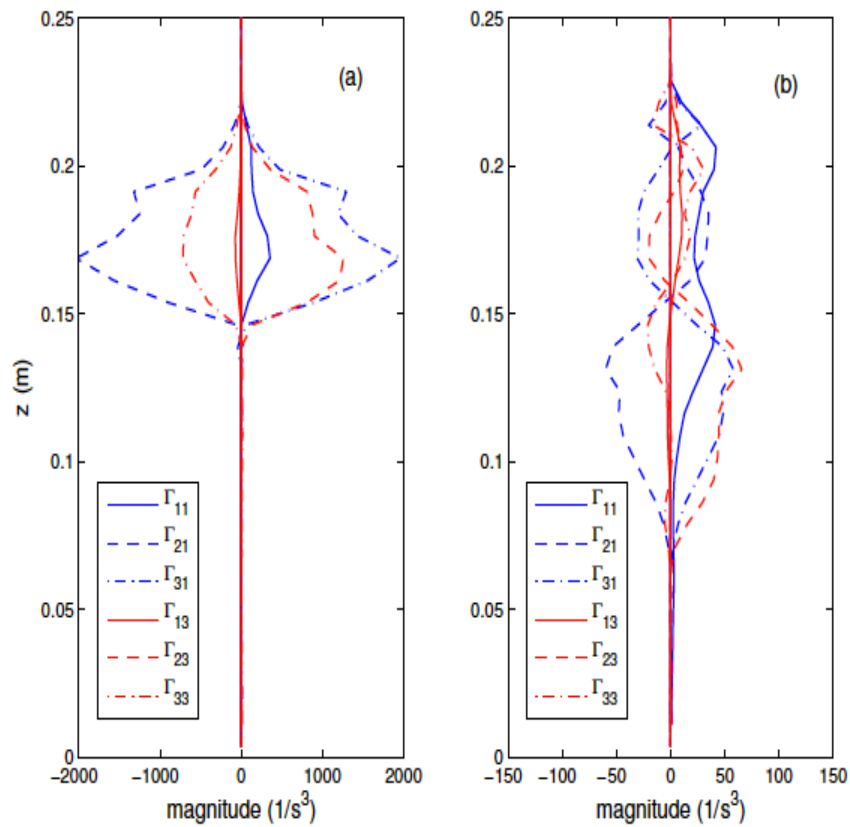
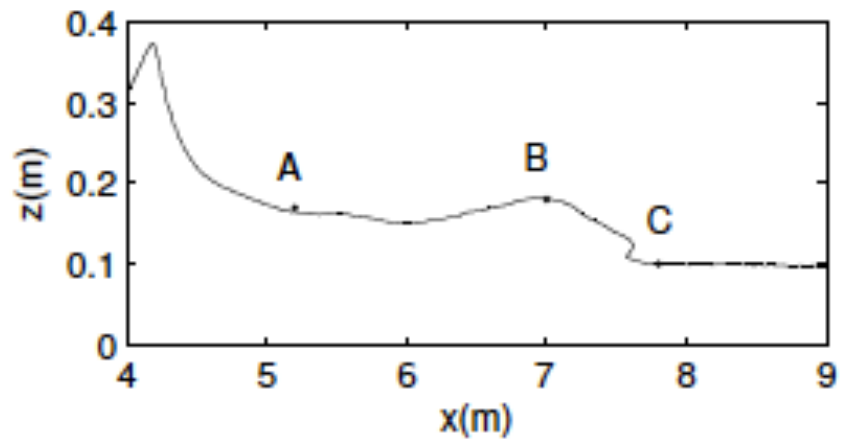
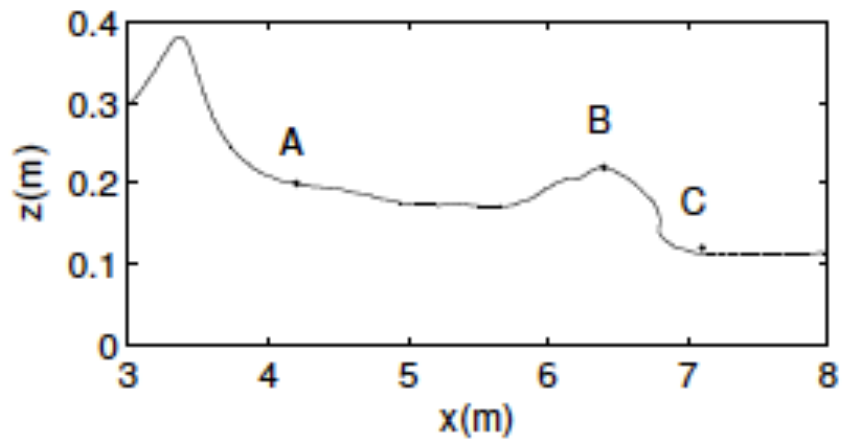
Detection of vortex tilting

- Enstrophy production

$$\frac{D(\frac{1}{2}\omega_i\omega_i)}{Dt} = \omega_i\omega_j \frac{\partial u_i}{\partial x_j} + \nu \frac{\partial^2(\frac{1}{2}\omega_i\omega_i)}{\partial x_j \partial x_j} - \nu \frac{\partial \omega_i}{\partial x_j} \frac{\partial \omega_i}{\partial x_j}$$

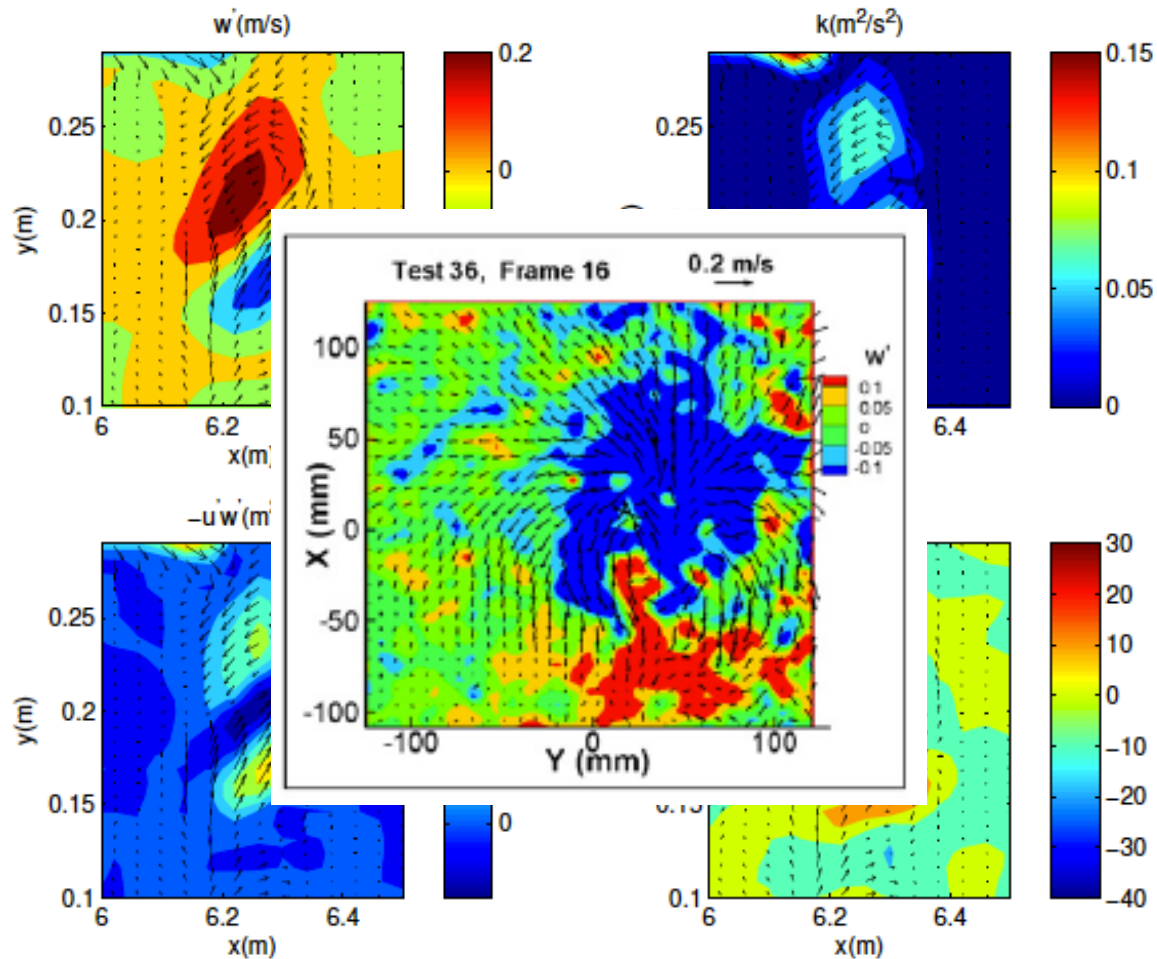
- Stretching and bending

$$\begin{aligned} \omega_i\omega_j \frac{\partial u_i}{\partial x_j} = & \underbrace{\omega_x\omega_x \frac{\partial u}{\partial x}}_{\Gamma_{11}} + \underbrace{\omega_x\omega_y \frac{\partial u}{\partial y}}_{\Gamma_{21}} + \underbrace{\omega_x\omega_z \frac{\partial u}{\partial z}}_{\Gamma_{31}} + \\ & \underbrace{\omega_y\omega_x \frac{\partial v}{\partial x}}_{\Gamma_{12}} + \underbrace{\omega_y\omega_y \frac{\partial v}{\partial y}}_{\Gamma_{22}} + \underbrace{\omega_y\omega_z \frac{\partial v}{\partial z}}_{\Gamma_{32}} + \\ & \underbrace{\omega_z\omega_x \frac{\partial w}{\partial x}}_{\Gamma_{31}} + \underbrace{\omega_z\omega_y \frac{\partial w}{\partial y}}_{\Gamma_{32}} + \underbrace{\omega_z\omega_z \frac{\partial w}{\partial z}}_{\Gamma_{33}} \end{aligned}$$

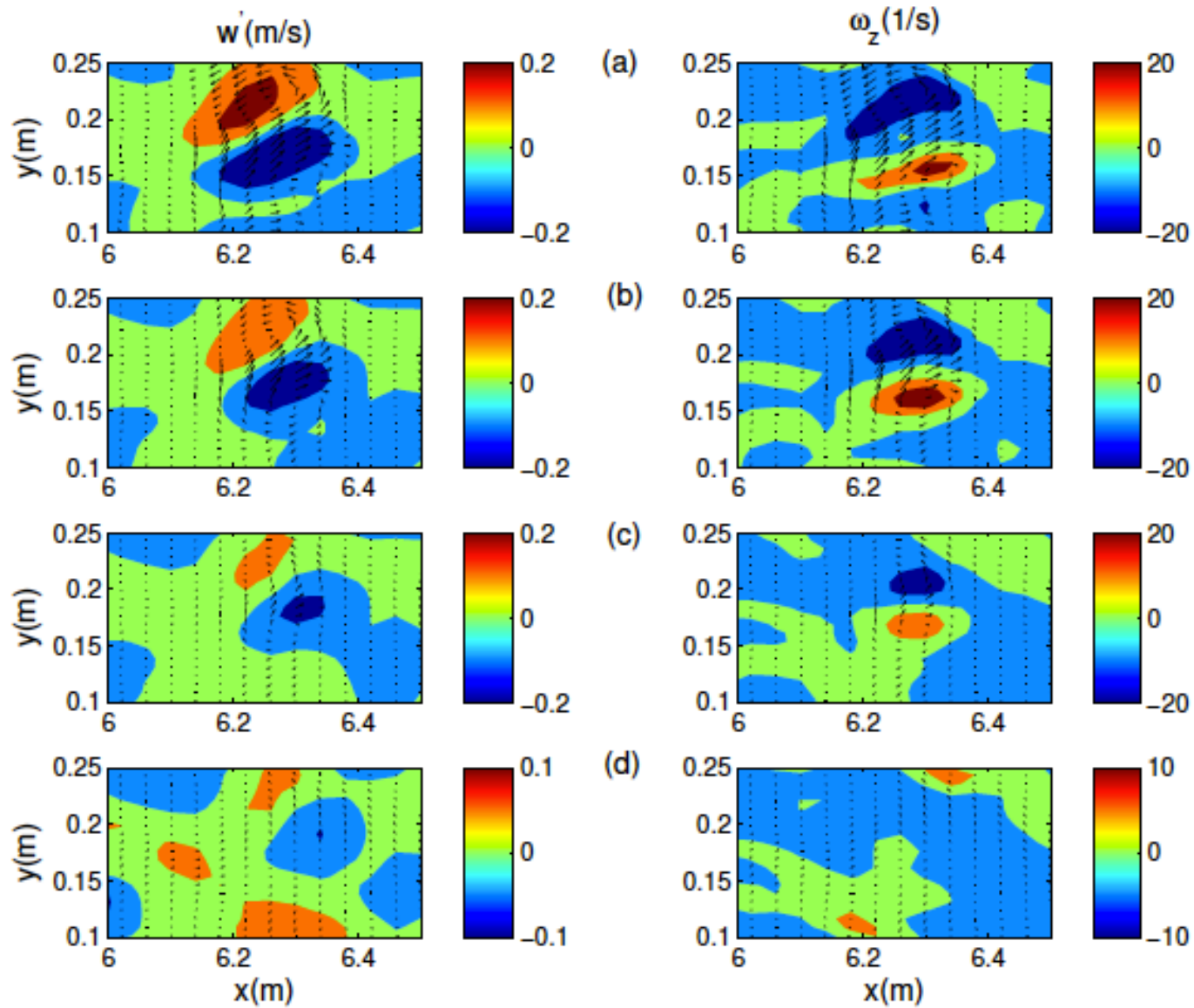


(a) crest region; (b) back face of breaking wave

Downburst of Turbulent Fluid

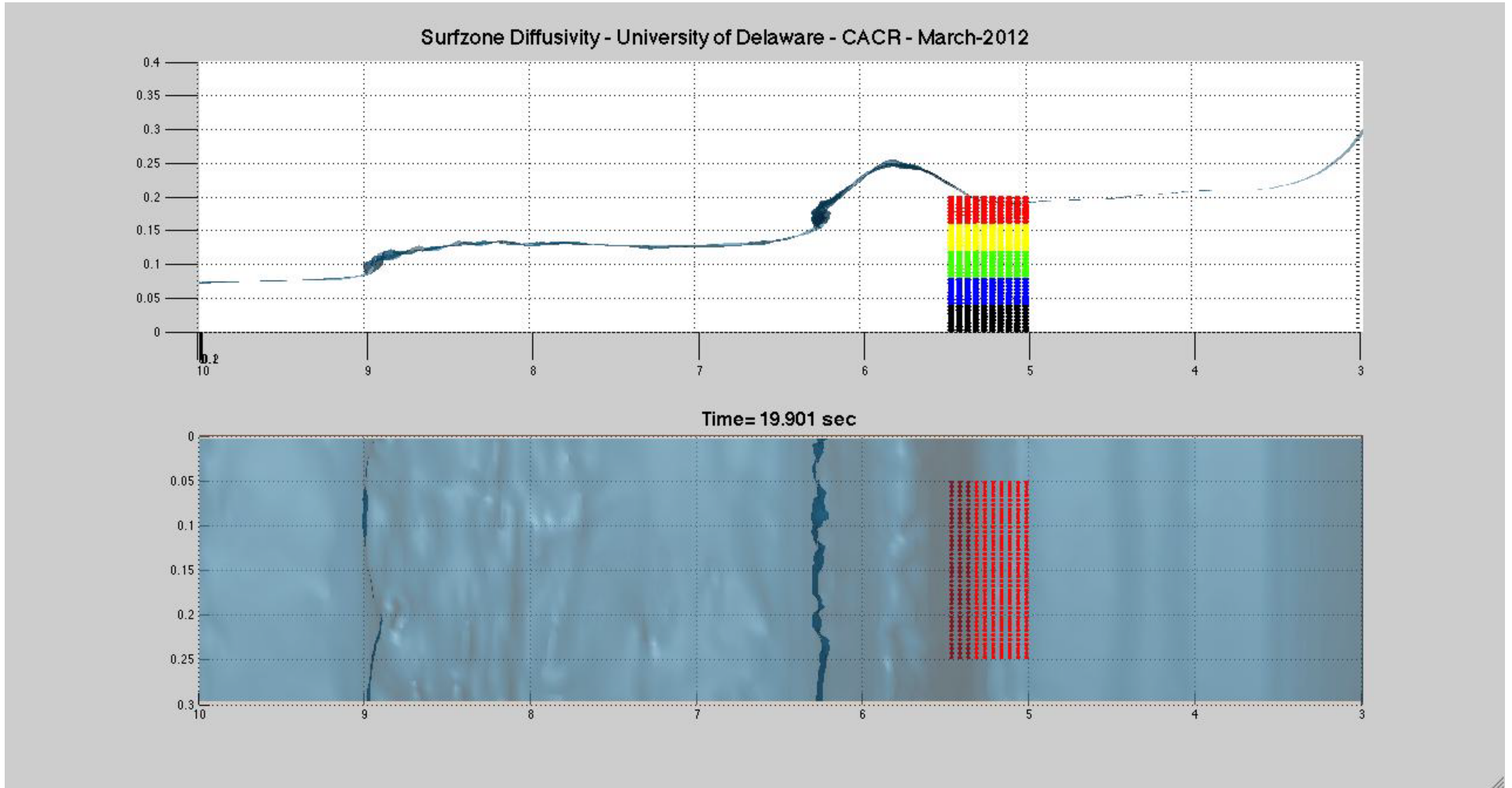


Instantaneous turbulent velocities, turbulent kinetic energy, Reynolds stress and vorticity in a downburst event in $t=t_b+5/8T$

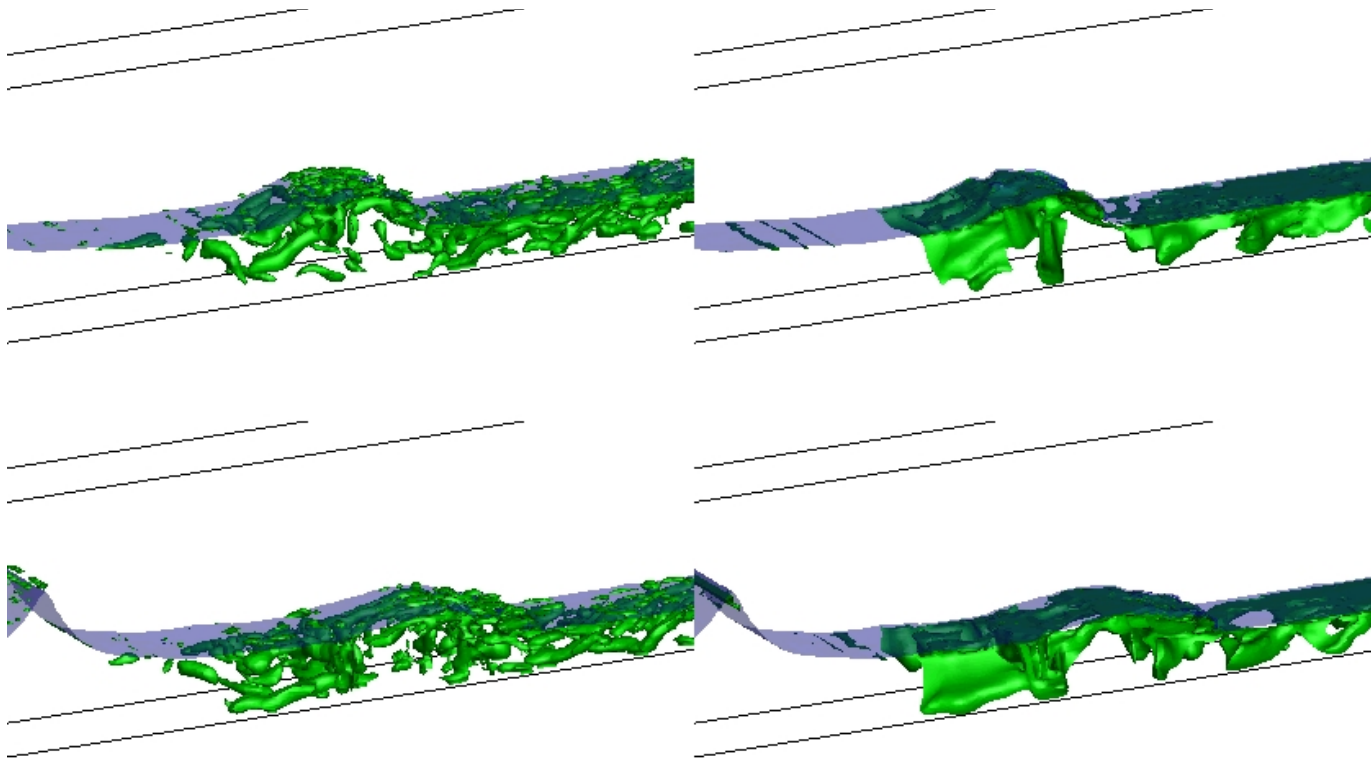


(a) $z=17$ cm; (b) $z=15$ cm; (c) $z=13$ cm; (d) $z=10$ cm

Lagrangian fluid particle tracking (liquid phase)

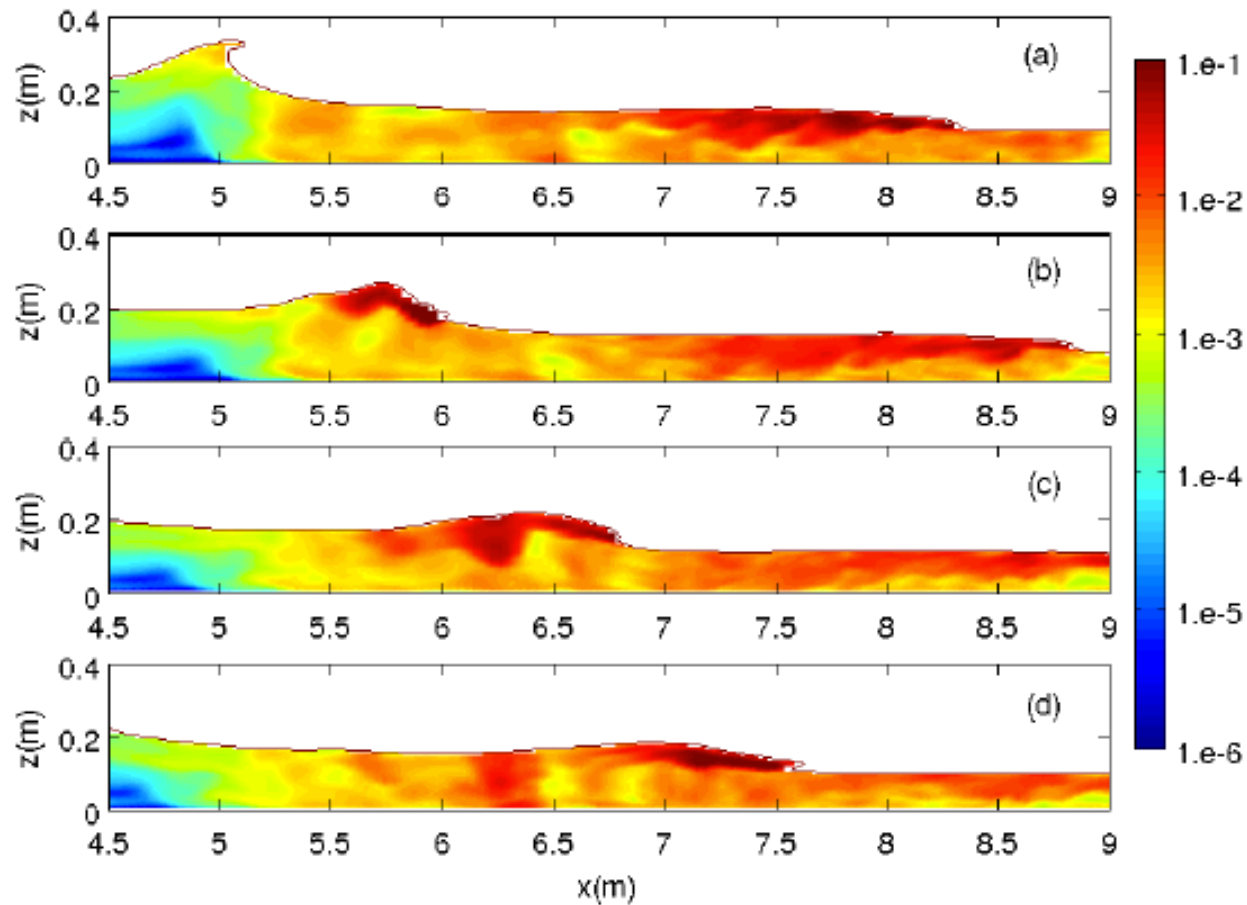


Interactions between Vortex Structures and Bubbles



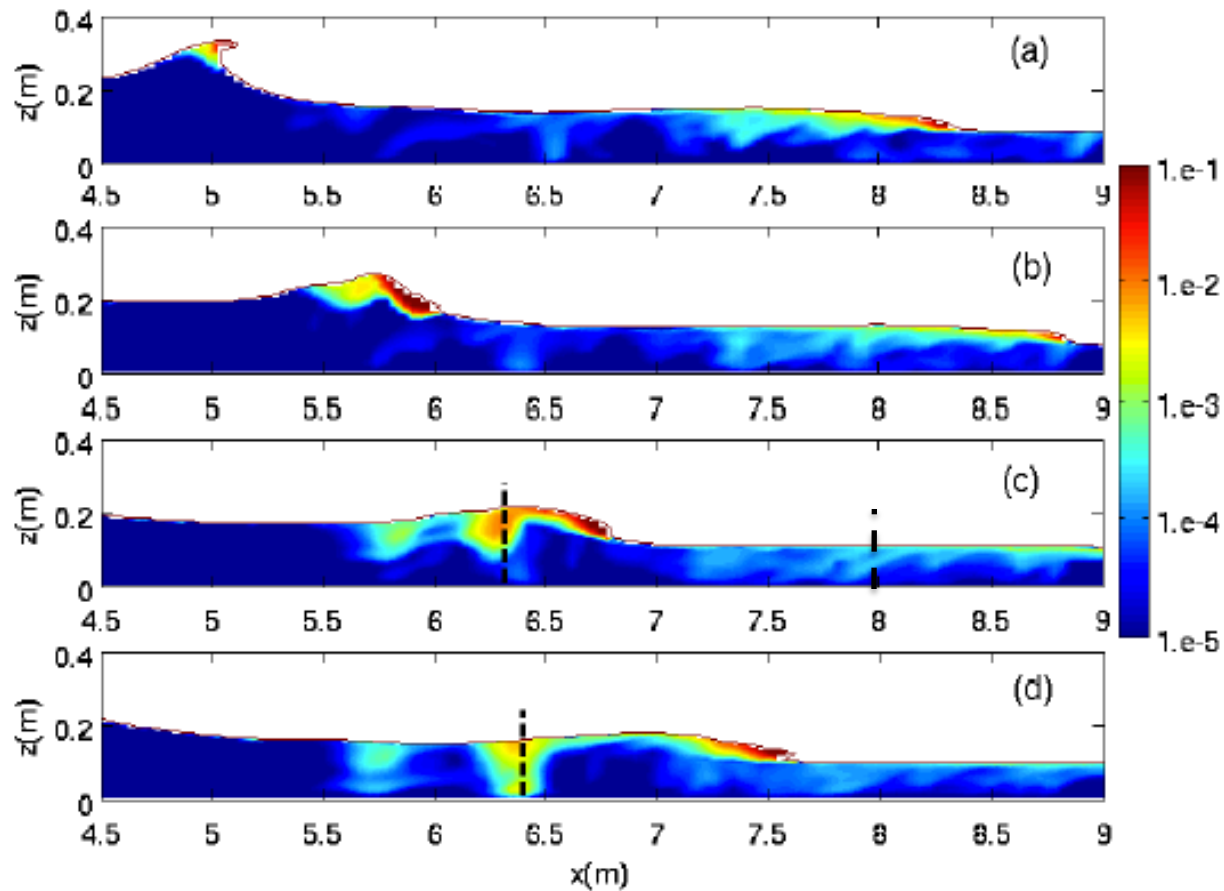
Vortex Structures (left panels) and void fraction distributions (right panels) at $t = t_b + 5/8T$ and $t = t_b + 7/8T$

Spanwise Averaged TKE



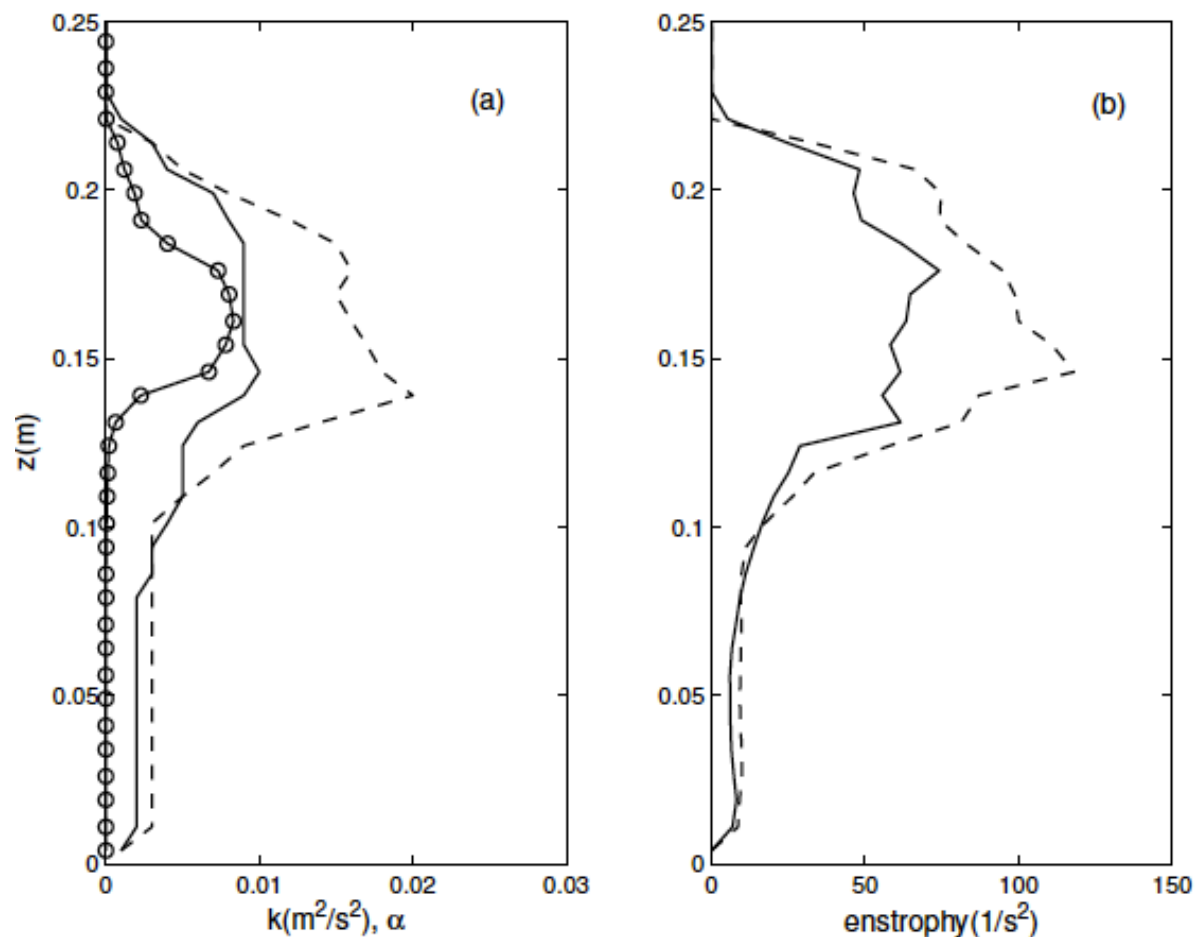
Spanwise averaged TKE at (a) $t=t_b+1/8T$; (b) $t=t_b+3/8T$;
(c) $t=t_b+5/8T$ and (d) $t=t_b+7/8T$.

Spanwise Averaged Void Fraction



Spanwise averaged void fraction at (a) $t = t_b + 1/8T$; (b) $t = t_b + 3/8T$; (c) $t = t_b + 5/8T$ and (d) $t = t_b + 7/8T$.

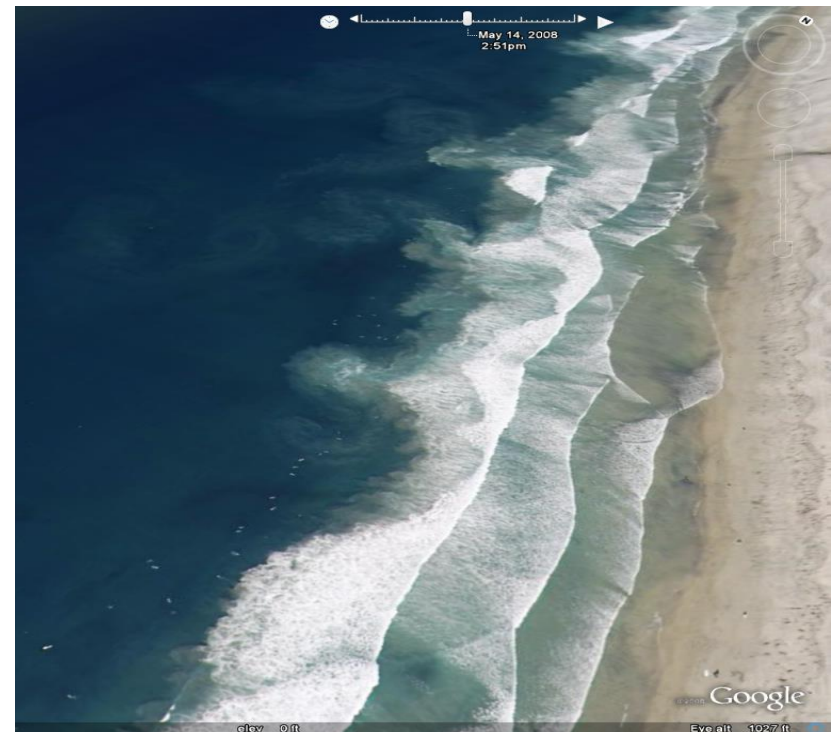
How do bubbles affect turbulence and vorticity field?



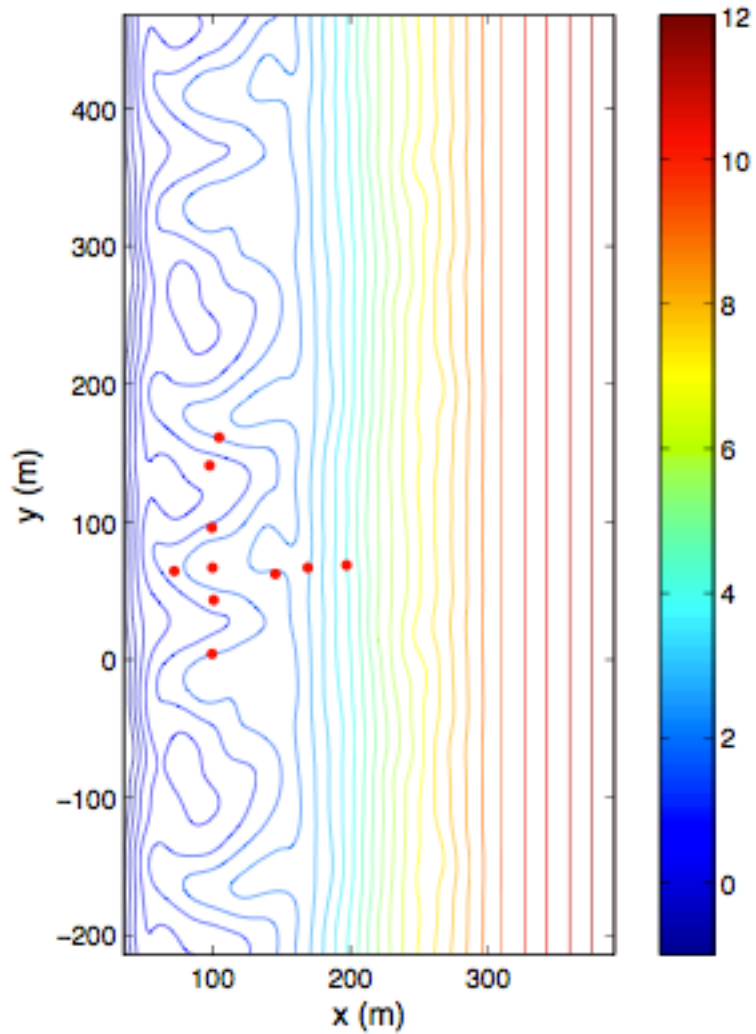
Zonal averaged turbulent kinetic energy and enstrophy with (solid line) and without (dashed line) bubbles

Apparent Surf Zone Dispersion

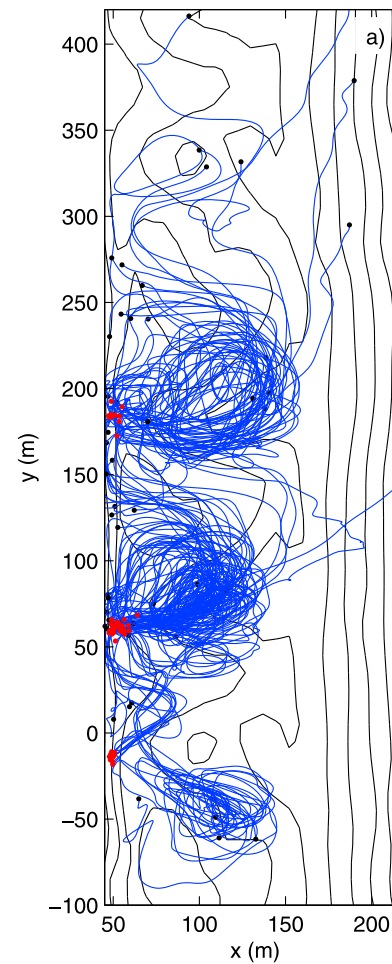
- Motivation: Need to explain early stages of lateral mixing processes in surfzone



Rip Current Experiment (RCEX) (MacMahan et al., 2010)

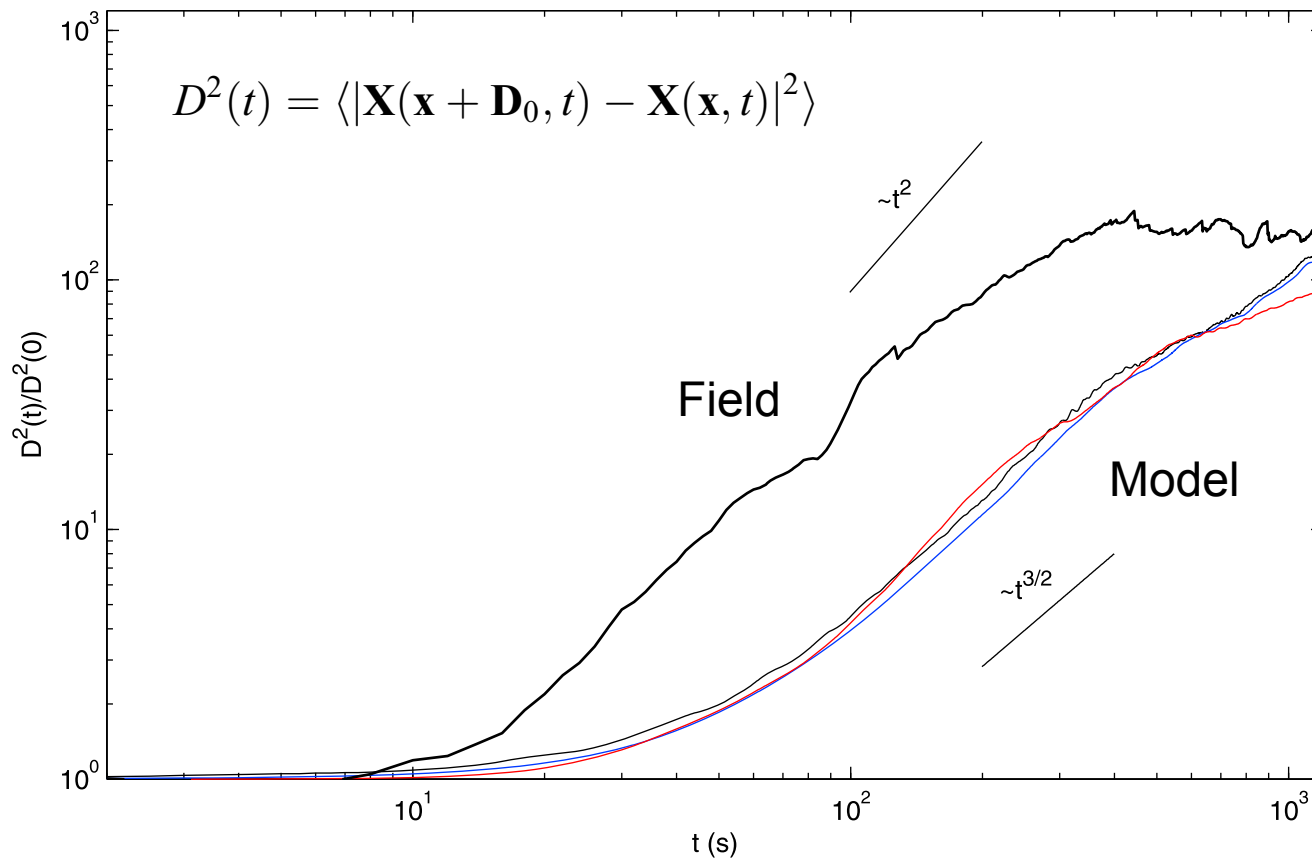


Bathymetry and instrument array

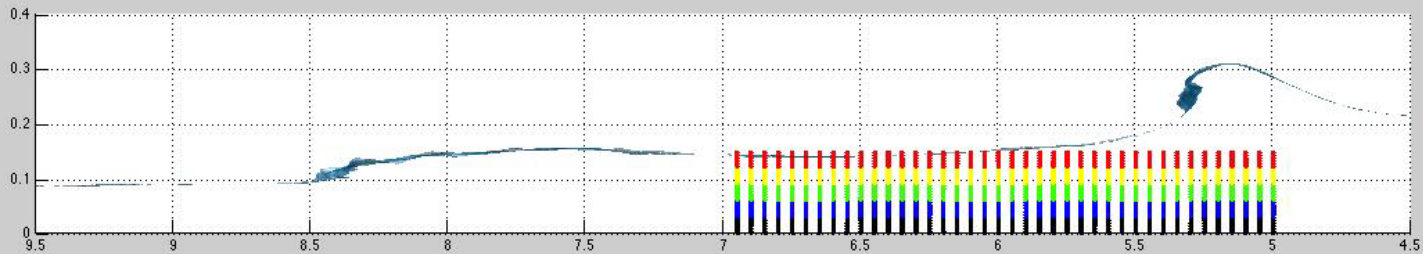
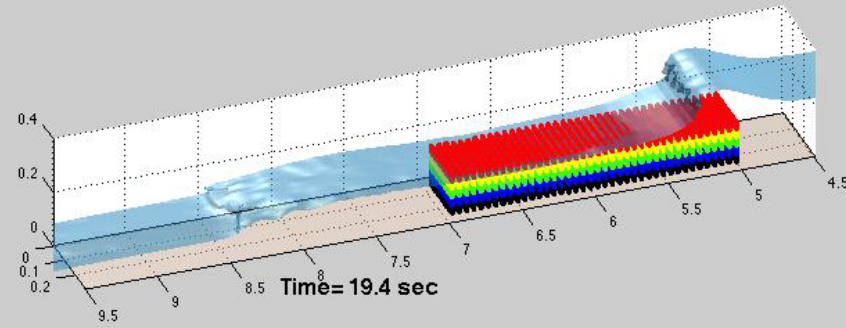


Observed GPS drifter trajectories

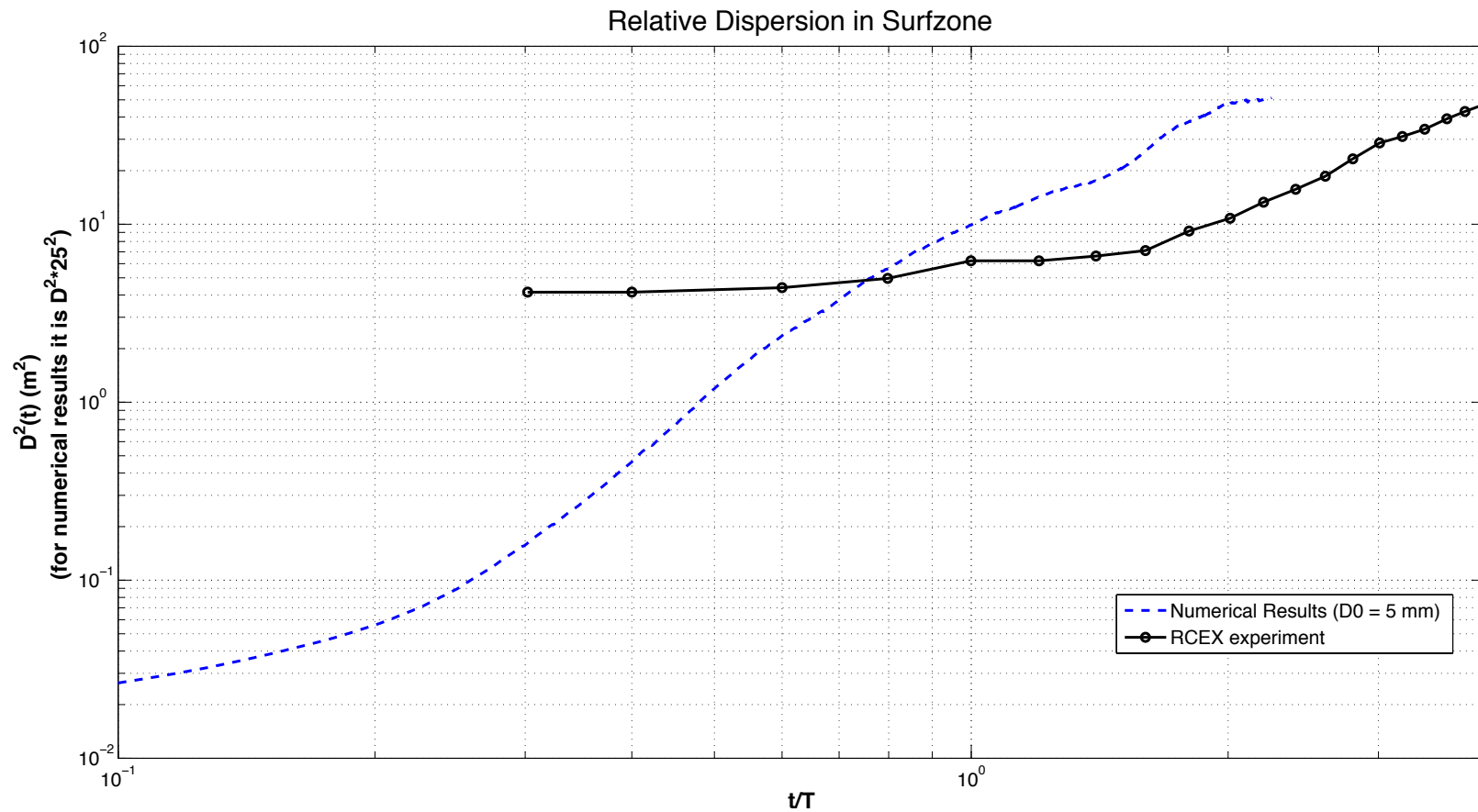
- Drifter trajectories simulated using wave-resolving and wave-averaged models
- Resulting two-point relative dispersion estimates agreed with each other but lagged behind field observation.



Two-point particle statistics based on Lagrangian particle tracking in multiphase simulation



Model results for short term relative dispersion



Future

- Foam production, transport and erosion at water surface
- Implementation of sediment phases
- Simulation of whitecap events in laterally unconstrained domains (application to the gas transfer problem)
- Attack the problem of the initial development of bubble population during cavity collapse
- Better comparisons to available field observations
- Incorporation of oil droplets in the formulation